Tampereen yliopisto

Salla Hartikainen

RECYCLED UHMWPE AND GREEN VALUES FOR APPLICATIONS OF LOW CONTACT FRICTION

Master of Science Thesis
Faculty of Engineering and Natural Sciences
Examiner: Mikko Kanerva
Examiner: Ilari Jönkkäri
April 2022

ABSTRACT

Salla Hartikainen: Recycled UHMWPE and green values for applications of low contact friction
Master of Science Thesis
Tampere University
Master's Degree Programme in Material Science
April 2022

The objective of the thesis is to find alternative materials for a snowmobile's sliding parts. The wearable part is sliding against steel in the application thus it should have good sliding properties as well as good wear resistance and operate well in extreme conditions, particularly in cold conditions. The reference material currently in use is ultra-high-molecular-weight polyethylene (UHMWPE). The optional materials were selected paying attention to the environmental perspective as well as the performance of the material. Materials selected as alternative materials included recycled grades of UHMWPE of two manufacturers as well as polyimide, which was selected due to its material performance. The alternative materials of recycled UHMWPE correspond more the reference material but are more environmentally sustainable and more cost effective compared to the reference material. Whereas polyimide is a high-performance plastic meaning higher costs.

The reference material and the alternative materials were tested to compare and select the most suitable material for the application. The tests included tensile testing, dynamic mechanical analysis (DMA) and pin-on-disk tests. In the tests the mechanical properties such as modulus, tensile strength and elongation were tested, as well as the effect of temperature on modulus and coefficient of friction were compared.

The results show that polyimide has superior mechanical properties compared to the other materials. However, coefficient of friction of polyimide was the highest of the materials making it perform the worst in the friction testing. The recycled alternatives performed well in comparison to the reference material. The lowest coefficient of friction was measured with one of the recycled materials. Recycled UHMWPE had also slightly higher storage modulus in the DMA analysis compared to the reference material. The recycled UHMWPE is cost effective and environmentally more sustainable due to the recycled nature. In conclusion, recycled UHMWPE would be the most suitable replacement material for the original virgin UHMWPE material.

Keywords: ultra-high-molecular-weight polyethylene, UHMWPE, polyimide, recycled, tensile test, DMA, pin-on-disk, coefficient of friction

TIIVISTELMÄ

Salla Hartikainen: Green Values in Wearable Parts in Structural Applications For Thermoplastics
Diplomityö
Tampereen Yliopisto
Materiaalitekniikan diplomi-insinöörin tutkinto-ohjelma
Huhtikuu 2022

Diplomityön tavoite on löytää vaihtoehtoinen materiaali moottorikelkan liukumuoviksi. Tämä liukumuovi on kuluva osa, joka liukuu teräsosaa vasten, joten valitulla materiaalilla täytyy olla hyvät liukuominaisuudet sekä hyvä kulutuskestävyys. Lisäksi materiaalin täytyy toimia hyvin äärriolosuhteissa, erityisesti kylmissä olosuhteissa. Referenssimateriaali, joka tällä hetkellä on käytössä, on ultrasuurimolekyylinen polyeteeni (UHMWPE). Vaihtoehtoiset materiaalit valittiin kiinnittäen huomiota ympäristönäkökulmiin sekä materiaalin suorituskykyyn. Materiaalit, jotka valittiin vaihtoehtoisiksi materiaaleiksi ovat kierrätetty UHMWPE kahdelta eri valmistajalta, sekä polyimidi, joka valittiin hyvien materiaaliominaisuuksiensa ansiosta. Näistä kierrätetyt UHMWPE materiaalit vastaavat enemmän alkuperäistä referenssimateriaalia, mutta ovat ympäristön kannalta kestävämpiä sekä edullisempia. Sen sijaan polyimidi on erittäin suorituskykyinen mutta kalliimpi vaihtoehto.

Referenssimateriaalilla sekä vaihtoehtoisilla materiaaleilla tehtiin testejä, jotta voitiin verrata materiaaleja keskenään sekä valita paras vaihtoehto applikaatioon. Testit sisälsivät vetokokeet, DMA:n ja pin-on-disk testit. Testeissä verrattiin materiaalien mekaanisia ominaisuuksia, kuten moduulia, vetolujuutta sekä venymää. Lisäksi verrattiin lämpötilan vaikutusta moduuliin, sekä kitkakerrointa.

Tulokset kertovat, että polyimidillä on ylivoimaiset mekaaniset ominaisuudet verrattuna muihin materiaaleihin. Kuitenkin polyimidin kitkakerroin on korkein, eli se pärjäsi huonoiten kitkatesteissä. Kierrätetyt vaihtoehdot suoriutuivat hyvin verrattuna referenssimateriaaliin. Alhaisin kitkakerroin mitattiin kierrätetyllä materiaalilla. Kierrätetyllä UHMWPE:llä oli myös hieman korkeampi varastomoduuli DMA analyysissä verrattuna referenssi materiaaliin. Kierrätetty UHMWPE on myös edullinen ja ympäristön kannalta kestävämpi vaihtoehto kierrätetyn sisältönsä ansiosta. Yhteenvetona voidaan sanoa, että kierrätetty UHMWPE olisi sopivin vaihtoehtoinen materiaali alkuperäiselle neitsyt UHMWPE materiaalille.

Avainsanat: ultrasuurimolekyylinen polyeteeni, UHMWPE, polyimidi, kierrätetty, vetokoe, DMA, pin-on-disk, kitkakerroin

PREFACE

I would like to thank the supervisors of the Master's thesis, Associate Professor Mikko Kanerva and University Instructor Ilari Jönkkäri for their good and close cooperation during the work. In addition, I would like to thank Olli Orell, Clara Lessa Belone and Farzin Javanshour for their good collaboration during the thesis project.

Tampereella, 14.4.2022

Salla Hartikainen

CONTENTS

LIST OF SYMBOLS AND ABBREVIATIONS

AFM	Atomic force microscopy
CO_2	Carbon dioxide
COF	Coefficient of friction
DA	Displacement amplitude
DMA	Dynamic mechanical analysis
FA	Force amplitude
FO	Force offset
GHG	Greenhouse gas
HDPE	High-density polyethylene
LCA	Life cycle assessment
PA66	Polyamide 66
PE	Polyethylene
PEEK	Polyether ether ketone
PI	Polyimide
PLA	Polylactic acid
POM	Polyoxymethylene
PMMA	Poly(methyl methacrylate)
PS	Polystyrene
PTFE	Polytetrafluoroethylene
PVA	Poly(vinyl alcohol)
PVC	Polyvinyl chloride
UHMWPE	Ultra-high molecular weight polyethylene
RCA	Real contact area
SEM	Scanning electron microscopy

°C	Degree of Celsius
μ	Coefficient of friction (COF)
σ	Stress
ε	Strain
A	Area
b	width
E	Activation energy
E’	Storage modulus
E’’	Loss modulus
E_s	Sample modulus
F	Force
G	The geometry factor
h	thickness
kJ	Kilo joule
l	Length
P	Pressure
R	Gas constant
rpm	Revolutions per minute
S_s	Sample stiffness
tan δ	Loss factor
T	Temperature
T_g	Glass transition temperature
T_m	Melting temperature
T_s	Sample temperature
T_{ca}	Clamp temperature
v	Velocity

1. INTRODUCTION

Nowadays, it has become more and more important to consider the environmental impact of a product. In one hand, the raw-material resources are not endless on Earth, and we need to consider how to utilize the available raw materials in the most effective manner. On the other hand, there is an increasing demand from the consumers to produce more environmentally sustainable products. These viewpoints in mind, the environmental impacts of the plastics used in our products need to be reassessed to ensure the sustainability of the products we produce and operate.

The sustainability of plastics is a widely acknowledged issue. Plastics are most often derived from non-renewable resources making them seem unsustainable by nature. 99 % of plastics produced are made by using fossil-based raw materials (Ita-Nagy et al., 2020). In any case, they have a profound place in today's material selection because of their exceptional characteristics combining availability, light-weightiness, cost-effectiveness, and easy machinability. There are hundreds of different plastic types with a wide range of characteristics to choose from. But how to select the best option for a particular application? Not to mention how to consider the environmental impacts of each choice.

The aim of the thesis is to find different options to replace UHMWPE material (UTEC6540) currently in use, to enhance the performance of the vehicle, and in addition to find more environmentally sustainable materials to replace virgin UHMWPE. Three options were selected: recycled UHMWPE (PE10000R) by Aikolon (Oulu, Finland) and recycled UHMWPE (Tivar) by Bay Plastics Ltd. (North Shields, Great Britain) was selected due to their recycled content and polyimide (Vespel) by DuPont material was selected because of its material performance in general.

The methods used in testing the mechanical and thermal properties of the materials were tensile testing, dynamic mechanical analysis (DMA) and pin-on-disk test. The tensile testing was conducted to gather general information about the material properties, such as Young's modulus. DMA was used to investigate the materials performance in different temperatures and when subjected to dynamic loading. Pin-on-disk test was used to measure the friction properties of the different material candidates.

The aim of the thesis is to compare the different tested material characteristics and to consider which of the materials would be most suitable for the application regarding the

test results, sustainability factors and costs. The aim is to test the materials in similar conditions as in real-life to achieve results which correlate the real-life application as well as possible. The operation temperature of the application ranges from -40°C to above 0°C and even up to room temperature. The mechanical behaviour of the material in different temperatures is of interest when considering the material performance in real-life.

When considering the coefficient of friction (COF), this factor is not a material constant, but always depends on the system. The factors affecting COF include the material couple, the contact surface, load, speed, lubrication, and temperature. The system is always a combination of those factors, and it is challenging to control precisely all those factors. The test is always only a simulation of the real-life conditions and never completely achieves the real-life conditions. However, in this thesis, the focus is on comparing the material candidates with each other to select the most suitable material for the application as well as to study the effects of recycling on UHMWPE.

2. THEORETHICAL BACKGROUND

2.1 Environmental impacts of plastics

One thing to help with assessing the sustainability of certain plastic is to look at its life cycle. The life cycle of a plastic product includes the following steps: extraction, production, fabrication, use and end-of-life. The end-of-life for plastics can mean landfill, energy recovery or recycling. There are a lot of steps which must be considered separately to get a full understanding of the sustainability of certain plastic. It is very challenging to gather the needed information from every step if the information is available in the first place. This kind of assessment requires a lot of time and detective work to conduct, thus this is not possible to perform in the given time period. Instead of assessing the whole life cycle, a more qualitative approach is taken in assessing the sustainable options for this application. (Alhazmi et al., 2021)

In general, the environmentally sustainable options for plastics available on the markets include recyclable, recycled, biobased and biodegradable materials. These categorizations are used as the starting point in selecting sustainable materials to replace the current one used in the application considered in this thesis.

First, let's consider recycled plastics. Recycling plastic waste can be divided into primary, secondary, and tertiary recycling categories. The primary recycling includes plastic waste discarded in the industry, for instance parts that are machined causes homogenous industrial waste. Secondary recycling includes the mechanical recycling of recovered plastics from consumers. Tertiary recycling includes chemical recycling, often pyrolysis or hydrolysis processes where the plastic is broken down into monomers, which are further used as raw material for plastic production. Recycling of plastics often decreases the quality of the material, therefore there is always downgrading of the material, and it cannot be used in high-performance applications and the material cannot be recycled infinitely. Recycling only delays the final disposal of the plastic. On the other hand, it reduces the need to use virgin materials. (Alhazmi et al., 2021) (Ita-Nagy et al., 2020)

When discussing recyclability of virgin material, the sustainability of material is increased by recycling material after operational lifetime. To ensure high-quality secondary raw material, recycled material must be pure in terms of plastic type and contaminants. This can be achieved by improving the waste management systems. In addition, when materials are selected for specific application, they should consist of one plastic type to be

able to recycle them effectively and to produce a high-quality secondary raw material from the waste.

Secondly, biobased materials shall be discussed; biobased plastics can be divided into two categories: first generation bioplastics and second-generation bioplastics. First generation bioplastics are synthesized of crop which can be consumed by humans and animals and are rich in carbohydrates, e.g., sugarcane, corn, or wheat, as a raw material. The raw material for second generation bioplastics comes from crops not suitable for food or feedstock. For instance, bagasse, grass, or wood are considered as a raw material for second generation bioplastics. (Kikuchi et al., 2013)

A review by Ita-Nagy et al. (2020) discusses the challenges concerning biobased plastics. Using biobased plastics instead of fossil-based plastics has some environmental concerns: for instance, the generation and handling of raw material can cause problems due to limited land use capacity. Displacement of food production, decrease in biodiversity and deforestation causing more greenhouse gas (GHG) emissions. The results of the review indicate that biobased plastics are more beneficial compared to fossil-based plastics in relation to climate change. However, acidification, photochemical ozone formation and eutrophication have higher impacts on the environment in biobased materials due to harvesting techniques and the use of fertilizers and pesticides. (Ita-Nagy et al., 2020)

In the study by Kikuchi et al. (2013), life cycle assessment (LCA) was applied to biopolyethylene (bio-PE) and fossil-polyethylene (fossil-PE). The study showed, that GHG emissions of bio-PE were 1,26 CO_2 cq/kg compared to fossil-PE, which had GHG emissions of 5,1 CO_2 cq/kg. However, concerning acidification and eutrophication, bio-PE has 1,6 to 2 times higher impacts on the environment compared to fossil-PE. Agricultural practices have also impact on the environmental impacts. Depending on the harvesting techniques and the use of fertilizers of organic farming practices, the negative impacts on the environment can be decreased. (Kikuchi et al., 2013)

Another option to increase the sustainability of the plastic product is to use biodegradable materials. Biodegradable materials include for instance bio-based plastics such as polylactic acid (PLA) and oil-based plastics such as poly(vinyl alcohol) (PVA). These plastics can be processed after usage in an appropriate compost. For instance, plastics with ISO standard 14855 are compostable under controlled conditions. (ISO, 2018)

2.2 Tribological behaviour of plastics against steel

There are generally two phenomena affecting friction: adhesion and deformation. For polymeric materials, usually adhesion plays a greater role in friction. Adhesion bond can be formed by movement and orientation of the polymeric chains, or by direct interaction of polymer and coupling surface with different forces including covalent, ionic and Van der Waals forces. Covalent forces are effective at shorter distances (<0,5 nm), while ionic and Van de Waals forces are effective at distances approximately 1 to 100 nm. The deformation phenomena are described as the polymer's resistance to plouding. (Myshkin et al., 2009)

The factors affecting friction include adhesive junctions, shear, and rupture of rubbing materials and real contact area (RCA). Friction forces are the result of junctions sheared under applied tangential force. (Myshkin et al., 2009)

The external factors affecting friction in a system include the applied load, sliding velocity and temperature. The effect of applied load varies with the amount of load. At moderate loads (0,02-1 N) coefficient of friction (COF) has been found to decrease with increasing loads. This is due to elastic deformation of the surface asperities. At higher loads (above ~100 N) the COF has been found to increase with increasing loads due to plastic deformation of the asperities in contact. With loads from 10 to 100 N the COF is essentially constant at least for certain polymers, such as PTFE, PMMA, PVC, PE, and PA. (Myshkin et al., 2009)

Theoretically, the COF should not be dependent on sliding velocity. For polymers this applies if the temperature increase within the contact area is neglectable. In practice, the effect of temperature on friction is more complex and it is difficult to separate the effects of temperature and velocity on COF. When approaching the glass transition temperature (T_g) of the polymer, there has been found a strong dependence of sliding velocity on COF. At temperatures well below T_g, the dependence of sliding velocity on COF is not noticeable. When considering the sliding velocities, at moderate velocities (0,01-1,0 cm/s or 0,0036 – 0,36 km/h) there is no dependence of velocity on COF at least for polymers such as PTFE, PE, PMMA and PS. At lower velocities, the viscous resistance increases with increasing velocity, which means that COF increases with increasing velocity. At higher velocities, the elastic behaviour is more dominant meaning that the dependence of COF on velocity is only minor, and COF decreases with increasing velocity. (Myshkin et al., 2009)

Polymers are sensitive to frictional heating. The heating is generated due to deformation or from rupture of formed adhesive bonds. The effect of temperature on COF depends

on polymer, for instance for PE increasing temperature leads to decreasing COF. (Myshkin et al., 2009)

According to Unal et al. (2004) a linear decrease in coefficient of friction with increasing applied pressure has been recorded in dry conditions on pin-on-disk against steel counterpart for thermoplastics such as ultra-high-molecular-weight polyethylene (UHMWPE), polyamide 66 (PA 66) and polyoxymethylene (POM). The lowest coefficient of friction was recorded with UHMWPE and POM. In the study conducted by Unal et al. (2004), the wear rates showed very little sensitivity to sliding velocity and applied pressure.

In research conducted by Unal et al. (2014), the sliding velocity was found to have the strongest effect on the parameters of friction and wear. According to Wang & Li (1999), the sliding velocity has greater effect on wear behaviour compared to applied load in the case of UHMWPE. In some cases, it has been recorded, that with increasing applied load the coefficient of friction decreases. This can be explained by the rising temperature of the surface due to frictional heating, which causes the polymer to soften dramatically and to transfer a layer on the steel making the contact surface polymer-on-polymer which causes the lower friction coefficient. (Unal et al., 2014)

At rubbery state of polymer - above T_g - viscoelastic deformation happen due to thermal agitation and presence of free volume in the polymer. The rearranging of chains and rotation of bonds occur. When temperature decreases, there is a linear decrease in specific volume until there is no more free volume left between the chains. Below T_g, the polymer is stiff, and deformation is more elastic. (Jackson, 2012)

2.3 Tribological behaviour of plastic on ice

There has been research on the friction coefficient of polymers when sliding on ice. According to Baürle et al. (2015), the low kinetic friction coefficients when sliding on ice is due to a water film forming between the polymer and the ice. The thickness of the water film is proportional to the friction coefficient. The water film is generated by frictional heating. The friction coefficient is affected by temperature, sliding velocity, load, and apparent contact area. In addition, the thermal conductivity of the polymer has an effect on the level of friction. Insulated materials have lower friction coefficients compared to highly conducting materials. This is due to the phenomena, that frictional heating of insulating materials is conducted to surface of material and into the ice causing the ice to melt. (Baürle et al. 2015)

There have been found two mechanisms affecting coefficient of friction. On one hand, thicker water film leads to lower friction coefficient, but on the other hand, more water

between the sliding material and ice lead to increase in real contact area resulting in a higher friction coefficient. (Baürle et al. 2015)

Temperature plays a large role in sliding conditions. At low temperatures (T < -10°C) the frictional heat conducted on ice has little effect on melting the ice, therefore the water film formed is relatively thin, some microns thick. This regime is also called 'dry-to-boundary' friction (Stamboulides et al., 2012). At low temperatures, the effect of increasing velocity decreased friction coefficient due to increasing frictional heat conducted on ice causing more ice to melt and enabling a thicker water film to form between ice and sliding material. The effect of increasing load at low temperatures is that increasing load increase friction coefficient linearly due to larger apparent contact area. (Baürle et al. 2015)

At intermediate temperatures (-10°C < T < -1°C) the surfaces experience so called 'mixed friction', where the water film thickness is generally less than the roughness of the surface of ice, but solid-to-solid contact is decreased causing lower friction (Stamboulides et al., 2012). At intermediate temperatures, the friction coefficient does not seem to depend on velocity, even though temperature on sliding material does depend on velocity. A large amount of frictional heating is conducted on ice causing the ice to melt. The melting ice results in a thicker water layer. However, the effect of thicker water layer on friction coefficient is balanced by an increase in real contact area between ice and sliding material. (Baürle et al. 2015)

At temperatures close to melting point (T > -1°C), the friction coefficient is high due to significant increase in real contact area between the ice and the sliding material. The thickness of water layer is generally greater than the surface roughness. This regime is also called 'hydrodynamic friction' regime (Stamboulides et al., 2012). The increase in real contact can be explained by the increasing thickness of the water layer due to increasing temperature. The friction coefficient is dependent on velocity and load. Friction decreases as load increases due to increasing frictional heat leading to thicker water film and lower friction. (Baürle et al., 2015)

2.4 Testing and characterisation of wearable contact plastics

2.4.1 Tensile Testing

Tensile testing is used to determine the mechanical properties such as stiffness, toughness, brittleness of plastics. A stress-strain curve is formulated from the results, where stress is presented as a function of strain. The stress-strain curve shows the materials

response to applied stress, in this case for tensile stress. Engineering stress (σ) is defined as force (F) divided by the cross-sectional area (A):

$$\sigma = \frac{F}{A} \quad (1)$$

Engineering strain (ε) is defined as the change in length divided by the original length:

$$\varepsilon = \frac{\Delta L}{L_0} \quad (2)$$

(Kuhn et al., 2000)

Figure 1 presents a typical stress-strain curve for a polymeric material. At arrow in point *a*, curve is linear indicating that the deformation is elastic. Elastic deformation is reversible, which means that if the load is removed the material goes back to its original shape. At arrow of point *b* the material reaches its yield point, from which onwards, plastic deformation takes please. Plastic deformation is irreversible, and the material is deformed permanently. After the yield point necking occurs when nominal stresses fall after yielding. (Kuhn et al., 2000)

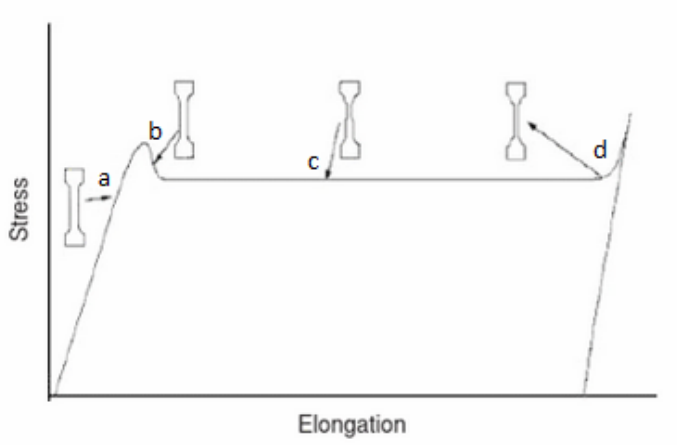

Figure 1. Typical stress-strain curve for polymers. (Hosford, 2010)

When considering what happens to the polymer in a molecular level while tensile testing, at arrow in point *a* in Figure 1, first, in the amorphous regions of the material, the coils are randomly oriented. When strain is subjected on the material, the coils start to orientate in the direction of the stress. The elastic deformation happens due to stretching of Van der Waals bonds between the molecular chains and by rotation of covalent bonds (Hosford, 2010) . After the yield point in plastic deformation (arrow in point *c*) disentanglement of the chains starts to occur. This point in the stress-strain curve is called cold drawing. This can be seen in the stress-strain curve, as strain increases without increasing the stress. The orientation of the chains in direction of stress is called stress induced

crystallization. When this kind of crystallization happens, the material becomes more difficult to deform, and deformation is achieved with higher stresses, as seen in Figure 1, the point of arrow *d*. This is called strain hardening. If the material has high degree of crystallinity it breaks at significantly higher stresses compared to the yield point. (Kuhn et al., 2000)

In Figure 2, the difference between stress-strain curves and material characteristics are presented. Material under testing is brittle if there is only elastic deformation and elongation at break is less than 5 %. With a stiff material the elongation at break is between 5 % to 10 %. Hard materials have high resistance to deformation, and it undergoes both elastic and viscoplastic deformation. Whereas soft material has low resistance to deformation while showing both elastic and viscous deformation. Toughness of material is determined as the energy absorption before break, and this can be curated from the stress-strain curve by calculating the area below the stress-strain curve. Strength of material can be determined from the stress-strain curve as the maximum stress, which is often the stress at break. (Kuhn et al., 2000)

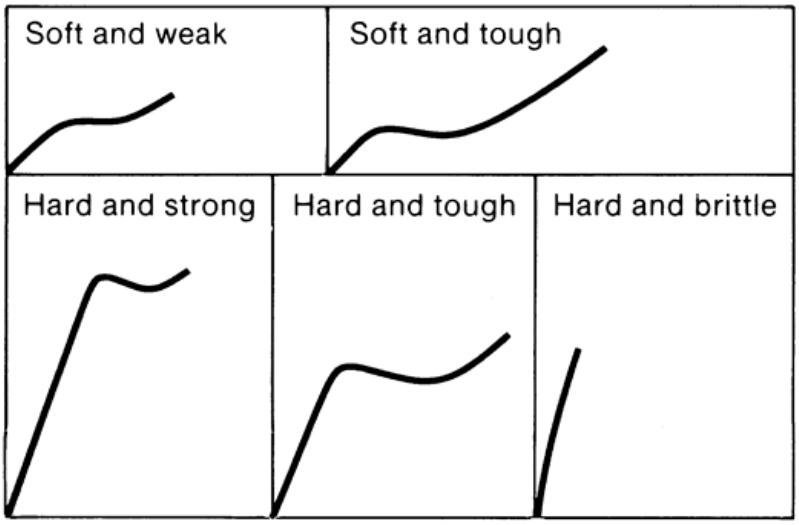

Figure 2. Tensile stress-strain curves for various materials. (Kuhn et al., 2000)

The shape of a tensile test specimen is shown in Figure 3. The specimen has typically wider ends, also called as the shoulders for gripping the specimen in the test device. The middle part is called the gauge section. The length of this section is typically four times the width of the gauge section. This part is where the deformation takes place. (Hosford, 2010)

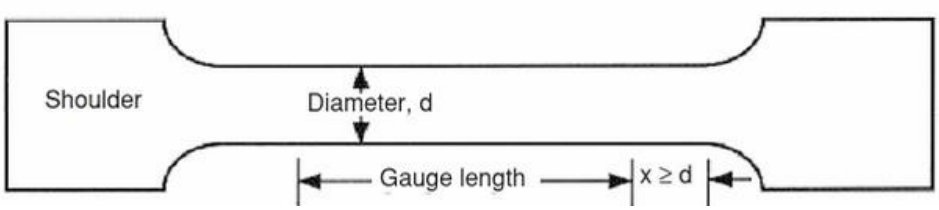

Figure 3. Typical tensile test specimen. (Hosford, 2010)

2.4.2 Dynamic Mechanical Analysis (DMA)

Dynamic Mechanical Analysis (DMA) is used to measure elastic and viscous properties of materials as a function of temperature, time, frequency, or stress. In the test, sinusoidal stress is applied in the specimen and the strain is measured to define Young's modulus. The method can be used to identify glass transition temperature (T_g) and other changes caused by molecular motion. DMA is also a useful tool in determining stiffness and dissipation of energy of the specimen. Stress is proportional to strain in small deformations, in which case the stress response is independent of strain rate. DMA is highly sensitive test device therefore it can be used in the so-called linear viscoelastic region. (Crompton, 2013)

The aim in this thesis is to determine the storage modulus in relation to changing temperatures. Storage modulus (E') corresponds to the elastic behaviour i.e., the stiffness of the material. The operation conditions of the application cover a wide range of temperatures from -40°C to above 0°C. The mechanical characteristics of the material in this temperature range are needed to be measured in this thesis. Storage modulus (E') describes the level of stiffness and it is proportional to the energy stored during one period under load. Storage modulus is calculated by the following formula:

$$E' = |E^*| cos\delta \quad (3)$$

(Mettler-Toledo AG, 2010a)

Other parameters derived from the measurement include loss modulus (E'') and loss factor (tan δ). Loss modulus (E'') determines the dissipated energy during dynamic loading. It is a measure for ability of material to follow deformation without breaking. Loss modulus is proportional to the work dissipated during one period under load. Loss modulus is calculated by the following formula:

$$E'' = |E^*| sin\delta \quad (4)$$

Loss factor (tan δ) characterizes the mechanical damping or internal friction of viscoelastic system. The peak value of tan δ is typically determined to find the maximum dissipation per frequency or temperature. The loss factor is calculated by using the following formula:

$$tan\delta = \frac{E''}{E'} \quad (5)$$

(Mettler-Toledo AG, 2010a)

The researched materials in this thesis are extremely stiff, thus 3-point bending fixture is used in the measurements. The sample dimensions are determined regarding the stiffness of the sample holder. The sample dimensions are selected according to the stiffness of the sample regarding the stiffness of the sample holder. The stiffness of the sample should be more than five times the stiffness of the sample holder. Sample stiffness (S_s) is calculated by using the following formula:

$$S_S = \frac{E_S}{g} \quad (6)$$

where, E_s is the Young's modulus of the sample and g is the geometry factor. The geometry factor (G) is calculated by the following formula:

$$G = \frac{l^3}{4 \times b \times h^3} \quad (7)$$

where l is the length of the sample, b is the width of the sample and h is the thickness of the sample. (Mettler-Toledo AG, 2010b)

2.4.3 Pin-on-Disk Measurement

The pin-on-disk test is a tribological test, which can be used to determine the coefficient of friction and wear rate of a material couple. The test can be done in varying controlled conditions. The parameters affecting the results include load, test speed, temperature, duration of test, surface roughness etc. Coefficient of friction (COF) can be described as the tangential resisting force acting at the interface between two objects. COF is not a material property, but a system property meaning, that the COF value depends highly on the conditions of the test. Wear can be described as the loss of material from contacting interface due to relative movement of two objects. (Dyson et al., 2020)

The variation of the test results is high due to the high effect of the many variables, therefore the comparison of representative values between studies is difficult. However, if the testing conditions remain similar, including the surface roughness of the material couples, comparison can be done. The aim of this thesis is to compare the friction forces

of different materials under controlled conditions. The different polymer materials are tested against a steel disk. The test conditions should resemble the real-life conditions as much as possible to get reliable results, which could be applied in the real application. (Dyson et al., 2020)

The pin-on-disk device consist of a pin, which is in this case a polymer rod, and a disk, in this case a steel one. The disk is rotating around its central axis at a constant rotational speed. The pin is pressed against the disk with a selected, constant load. The duration of the test is also set, and the sliding distance determined. To gain reliable results, repetitive tests are required. The relation of conditions to the results are complex, thus the conclusions made based on the results must be made with caution. (Dyson et al., 2020)

The wear rate can be analysed with several different methods, from rough measures of weight loss to more sophisticated methods including scanning electron microscopy (SEM) image analysis and atomic force microscopy (AFM). In this thesis, the wear rate is roughly observed from the height difference recorded during the measurement. (Dyson et al., 2020)

3. CANDIDATE MATERIALS

In this section, the material currently in use in the anticipated application and in addition the material options to replace the used material are presented. The material candidates selected include different types of ultra-high molecular weight polyethylene (UHMWPE): virgin and two recycled ones. The virgin material tested is UTEC6045 by Braskem and the recycled materials include PE1000R from Aikolon and Tivar 1000 R from Bay Plastics Ltd. In addition, a polyimide grade material was selected, in this case Vespel by DuPont. The mechanical and thermal properties of these materials are presented. In addition, the reasons why the material is selected are discussed in this chapter.

3.1 Ultra-High Molecular Weight Polyethylene (UHMWPE)

The reference material is Braskem's UTEC® 6540 Ultra-High Molecular Weight Polyethylene (UHMWPE), which is virgin material. The molecular weight of UTEC6540 is about $8{,}0 \times 10^6$ g/mol, which is about 10 times higher than molecular weight of high-density polyethylene (HDPE). The properties of UHMWPE include high abrasion wear resistance, high impact resistance and low coefficient of friction making the material self-lubricating. The material is also chemically resistant, thus can be used in corrosive or aggressive environments. The operating temperature range of UHMWPE is moderate of about -100°C to +82°C. (Braskem, 2018)

These properties enable the material to be used in high performance applications in a wide range of industries. Due to the self-lubricating property of the material, it can be used in sliding applications without any additional lubrication. The high abrasion wear resistance enables the material to be used as a replacement for metals providing a light-weight alternative to metals. (Braskem, 2016)

Processing of UHMWPE requires some special techniques because the material does not flow even above its melting point (133°C). RAM extrusion and compression moulding, or sintering (porous parts) can be used to process UHMWPE. In addition, machining techniques such as sawing, milling, planning, drilling, and turning can be applied. (Braskem, 2016)

In Table 1, the mechanical properties of UTEC6540 material are presented. The parameters that are of interest for the thesis are tensile strength at yield, which is >17 MPa, tensile strength at break, which is >30 MPa, elongation at break, which is 350 % and coefficient of friction, which is 0,09. (Braskem, 2018)

Table 1. Mechanical properties of Braskem UHMWPE UTEC6540. (Braskem, 2018)

Property	Method, Standard	Value
Density (g/cm^3)	ASTM D 792	0,925
Molecular weight (g/mol)	ASTM D 4020	$8{,}0\times10^6$
Melt temperature (C°)	-	133
Thermal expansion (1/C°)	ASTM D 696	$1{,}5\times10^{-4}$
Tensile strength at yield (MPa)	ASTM D 638	>17
Tensile strength at break (MPa)	ASTM D 638	>30
Elongation (%)	ASTM D 638	350
Impact strength (kJ/m^2)	ISO 11542-2, double notch	>100
Shore D hardness	ASTM D 2240, 15 sec	>58
Coefficient of friction, kinetic (against steel)	ASTM D 1894	0,09
Abrasion index (sand slurry)	Braskem internal, ISO 15527 reference set to 100	76

3.2 Recycled UHMWPE

The alternative materials selected as candidates to be researched include reprocessed UHMWPE, which consists of virgin UHMWPE and recycled UHMWPE. Reprocessed UHMWPE provide a more environmentally friendly and cost-effective material option to replace virgin UHMWPE. The price range of recycled UHMWPE is about 3-7 €/kg (Aikolon, 2019). The recycling of UHMWPE influences the mechanical properties of the material. During the recycling process there can occur some degradation of the material leading to slightly poorer quality of the product compared to virgin material. However, consumers of have not experienced any difference between reprocessed grades of UHMWPE compared to virgin grades of the same material. (Aikolon, 2019)

The recycled grades of UHMWPE tested were from Bay Plastics Ltd. (North Shields, Great Britain) (Tivar) and from Aikolon (Oulu, Finland) (PE1000R). The material properties of each plastic grade have been presented in Table 2 and Table 3. According to the manufacturer's websites, both grades of regenerated UHMWPE consist of mainly

recycled material with a portion of virgin material. The recycled material is by-product from a plastic factory's production line (Aikolon, 2019).

In Table 2, the mechanical properties of PE1000R material are presented. The parameters that are of interest for this thesis are Young's modulus, which is reported to be 900 MPa, tensile strength at break reported to be 27 MPa, elongation at break, which is reported to be 200 % and coefficient of friction, which is 0,2. (Wefapress, 2020)

Table 2. Mechanical properties of recycled UHMWPE PE1000R. (Wefapress, 2020)

Property	Method, standard	Value
Density (g/cm^3)	DIN EN ISO 1183	0,96
Molecular weight (g/mol)	-	~3-9x10^6
Tensile strength at break (MPa)	DIN EN ISO 527-2	27
Elongation at break (%)	DIN EN ISO 527	200
Flexural modulus (MPa)	DIN EN ISO 178	900
Modulus of elasticity	DIN EN ISO 527	900
Coefficient of friction (against steel)	-	0,2
Notched impact strength kJ/m^2	charpy, DIN EN ISO 179-1eA	>30-110
Toughness (Shore D) (Sh D)	DIN EN ISO 868	64–68
Wear resistance (%)	Sand Slurry method	~130
Melt temperature (C°)	-	130 - 135
Operating temperature max (C°)	-	80
Operating temperature min (C°)	-	-200
Dimensional stability under heat (C°)	DIN 53461 47	47
Vicat softening temperature (C°)	DIN EN ISO 306	79
Coefficient of thermal expansion, 23-100 °C (K^{-1})	DIN EN ISO 11359-1;2	2,0 × 10^{-4}
Specific heat capacity (J/(g×K))	ISO 22007-4:2008	1,8
Thermal conductivity (W/(m×K))	ISO 22007-4:2008	0,42
Moisture absorption (%)	-	< 0,01

In Table 3, the mechanical properties of Tivar material are presented. Young's modulus of Tivar has reported to be 700 MPa, tensile strength at yield to be 21 MPa and elongation at yield to be 11 %. (Bay Plastics Datasheet, 2022)

Table 3. Mechanical properties of recycled UHMWPE Tivar. (Bay Plastics Datasheet, 2022)

Property	Method, standard	Value
Density (g/cm³)	ISO 1183	0,93
Tensile strength at yield (MPa)	DIN EN ISO 527	21
Elongation at yield (%)	DIN EN ISO 527	11
Tensile modulus of elasticity (MPa)	DIN EN ISO	700
Impact strength (kJ/m^2)	DIN EN ISO 179	Without break
Ball indentation hardness (MPa)	DIN EN ISO 2039-1	38
Operating temperature max (C°)	-	80
Operating temperature min (C°)	-	-260
Mean coefficient of linear thermal expansion (K^{-1})	DIN 53752	1.8 x 10^{-4}

3.3 Polyimide

Polyimide is a high-performing plastic with excellent heat resistance. The material has a wide range of service temperatures ranging from -270°C to +300°C retaining its mechanical strength, creep resistance and dimensional accuracy. Polyimide has good chemical resistance, and it is inherently resistant to flame combustion. The material is processed by sintering due to its high mechanical stability even at elevated temperatures. Applications in which polyimide is used, include usage in electronic industry as insulating film, in demanding applications as constructive parts, bushings and bearings as well as in medical applications for instance as medical tubing. The mechanical properties of polyimide are listed in Table 4. Young's modulus of polyimide has reported to be 3600 MPa, tensile strength at break to be 116 MPa and elongation at break 3,8 %. (Aikolon, 2000)

Table 4. Mechanical properties of polyimide by Aikolon (Aikolon, 2000)

Property	Method, standard	Value
Density (g/cm^3)	DIN EN ISO 1183	1,34
Modulus of elasticity (tensile test) (MPa)	DIN EN ISO 527-1	3600
Tensile strength at break (Mpa)	DIN EN ISO 527-2	116
Elongation (%)	DIN EN ISO 527	3,8
Flexural modulus (MPa)	DIN EN ISO 178	3700
Notched impact strength kJ/m^2	charpy, DIN EN ISO 179-1eA	5
Toughness (Shore D)	DIN EN ISO 868	90
Operating temperature max (C°)		300
Operating temperature min (C°)		-270
Heat distortion temperature (C°)	DIN 53 461	368
Thermal expansion coefficient, 23-100 °C (10^{-5} K^{-1})	DIN EN ISO 11359-1;2	4,3
Specific heat capacity J/(g×K)	ISO 22007-4:2008	1,04
Thermal conductivity (W/(m×K))	ISO 22007-4:2008	0,22
Moisture absorption (%)	DIN EN ISO 62	1,08

Polyimide is a more expensive option with a price above 50e/kg, but the excellent material performance could reduce the costs in other sectors, such as in increasing the operating range and reducing energy consumption (Aikolon, 2000). The chemical structure of polyimide is presented in Figure 4.

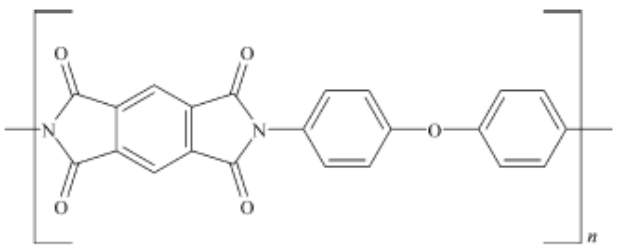

Figure 4. Typical chemical structure of polyimide. (McKeen, 2010)

4. METHODS

Three different mechanical and thermal testing methods were used to compare the three different types of materials selected to be candidate against the rival.

The methods used for testing the mechanical and thermal properties of the materials are tensile testing, dynamic mechanical thermal analysis (DMA) and pin-on-disk test. Tensile testing is used to compare the basic mechanical properties of the different materials, such as tensile Young's modulus, yield strength, elongation, and tensile strength at break. The DMA was used to test the effect of different temperatures on the mechanical behaviour of the materials. The pin-on-disk test was used to determinate the coefficient of friction of the different materials. A low coefficient of friction plays an important role in the sliding of the sliding parts against metal parts and has an effect also on the operating range of a vehicle with these parts.

4.1 Tensile testing and tensile specimens

The tensile tests were done by using model 5967 by Instron, tabletop universal testing device with a 500 N and 30 kN load cell. The 500 N load cell was used for UTEC6540, PE1000R and Tivar specimens and the 30 kN cell was used for polyimide specimens. A picture of the device is presented in Figure 5.

Figure 5. Electronic tabletop universal testing device with a 500 N load cell.

4.1.1 Tensile specimen preparation

The UTEC6540 specimens were machined from the from the real slider parts of the application vehicle. The sliders were first machined to 3 mm thick sheet and then a tensile testing punch was used to cut the ‘dog bone’ shaped specimens for the tensile testing. The dimensions of the specimens are presented in Figure 6. The PE1000R material was first machined into a 3 mm thick sheet and the tensile testing specimens were punched with the same tensile test ‘dog bone’ shaped punch as the UTEC6540 specimens. Tivar material was already a 3 mm thick sheet, from which specimens were punched. Six parallel specimens were prepared from UTEC6540, PE1000R and Tivar materials. The polyimide material was flattened to 3 mm thick sheet, from which two parallel specimens were sanded by hand to match the dog bone shape of the punched specimens. The specimens are presented in Figure 7.

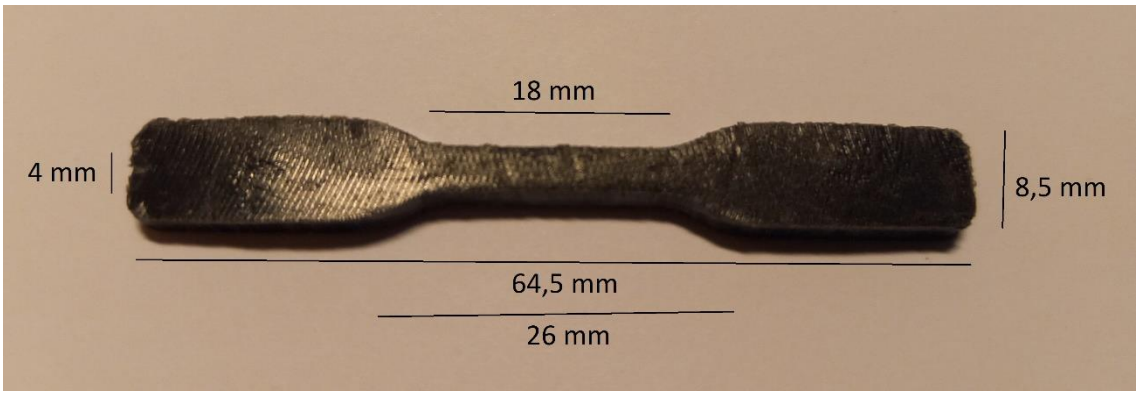

Figure 6. Dimensions of the tensile test specimens.

Figure 7. The tensile test specimens of UTEC6540, PE1000R, Tivar and Vespel, from left to right.

4.1.2 Measurement procedure

The testing rate was set to 5,0 mm/min. The tests were done at ambient conditions. Three parallel specimen were tested with UTEC6540, PE1000R and Tivar materials. Two parallel measurements were done with polyimide material due to material

limitations. The dimensions of the dog bone shaped samples are found in Figure 6. The approximate width of the samples was 4 mm and thickness was 3 mm. The initial length of the sample was 32 mm. The samples were loaded until breakage during testing.

4.2 Dynamic Mechanical Analysis (DMA) and samples

The Dynamic Mechanical Analysis was performed by using Dynamic Mechanical Analyser (DMA) DMA/SDTA861 (Mettler Toledo). The tests can be performed in three modes: shear, tension and three-point bending. For this thesis 3-point bending was selected due to its suitability for stiff materials. The force range of the device is from 5 mN to 40 N. The frequency range goes from 0,001 Hz to 300 Hz with three-point bending. Displacement range goes from 5 nm to 1,6 mm. The temperature range is from -100°C to 500 °C, but in practice the device could reach only -80°C. The cooling is achieved with liquid nitrogen. A picture of the DMA device is presented in Figure 8. (Tampere University, 2022)

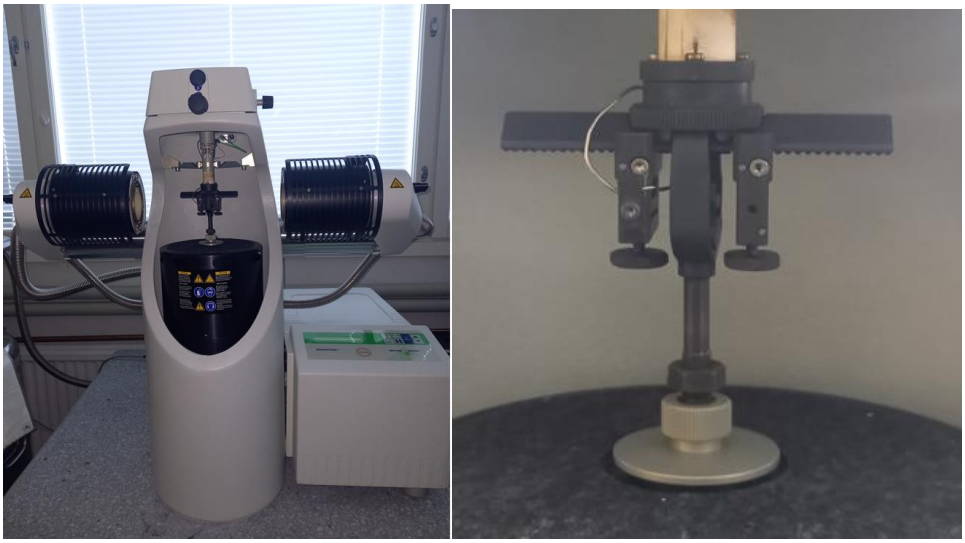

Figure 8. Dynamic Mechanical Analyser (DMA) DMA/SDTA861 (Mettler Toledo) with three-point bending set-up.

4.2.1 Sample preparation for DMA

The sample dimensions were selected by calculating the stiffness of the sample by using formula (6). The average flexural modulus of UHMWPE is 900 MPa and the geometry factor is calculated by using formula (7). The geometry factor for PE1000R was calculated to be 25 1/mm with sample dimensions of 30 mm × 10 mm × 3 mm. The sample stiffness resulted to be 36 N/mm, which is about 113 times smaller than the sample holder stiffness for 30 mm clamping length (4094 N/mm) presented in Table 5. For the

UTEC6540 sample the geometry factor was calculated to be 50,81 1/mm by using formula (7). The stiffness for UTEC6540 was calculated to be 17,7 N/mm according to formula (6), which is about 231 times lower than the sample holder stiffness when using 30 mm clamping length.

Table 5. Stiffness of the sample holder for different clamping lengths. (Thermal Analysis Application)

Clamping length (mm)	Sample holder stiffness (N/mm)
30	4094
40	2730
50	2464
60	2391
70	2181
80	1721

The sample dimensions were 38 mm × 10 mm × 3 mm according to the DMA device's criteria. The length of the sample itself was slightly longer than the clamping length to be able to clamp the samples to the sample holder properly. The samples for the DMA analysis are prepared by cutting from a machined sheet.

The UTEC6540 and PE1000R materials were first machined to 3 mm thick sheets. The Tivar material came as a pre-cut 3 mm sheet. The Vespel material came as a 20 mm diameter rod, from which 3 mm thick sheets were machined. The samples from the UTEC6540, PE1000R, Tivar and Vespel sheets were prepared with a circular saw, and the edges were finished with a carpet knife to get neat edges. Three parallel samples with dimensions of 38 mm in height, 10 mm in width and 3 mm in thickness were prepared. The pictures of the samples are shown in Figure 9.

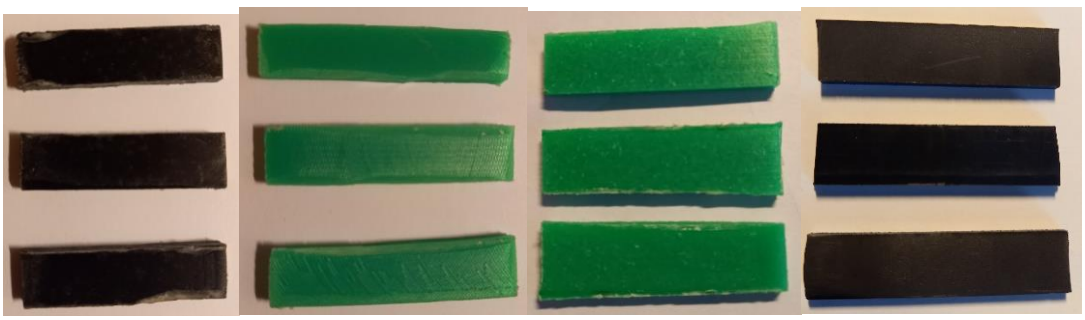

Figure 9. DMA samples of UTEC6540, PE1000R, Tivar and Vespel.

4.2.2 Measurement procedure for DMA

The test type chosen is 3-point bending because it is appropriate for stiff materials. The measurement is done with a temperature sweep with a set frequency of 10 Hz. The melting temperature of UHMWPE is 135 °C and in practice the minimum temperature reached with the device is -80 °C. The temperature range for UHMWPE samples is set to -55 °C to +120 °C. The minimum temperature the anticipated vehicle is operated in can go down to -40 °C, thus -55 °C was selected as a minimum temperature. The heating rate is set to 3 K/min.

The pre-tests are done before the actual measurements. First the force offset (FO) was determined at -25 °C and with frequency of 10 Hz. The test programme for force off-set was done initially in 10 segments between 1,5 N to 20 N.

After the force offset test, another pre-test was conducted to determine the force amplitude (FA) and displacement amplitude (DA). This test was done at -25 °C and with frequency of 10 Hz and with the determined force offset. From a Young's modulus versus displacement curve the end of linear region of displacement was determined and the force amplitude was chosen from a force-displacement curve.

4.3 Pin-on-Disk measurement and samples

The pin-on-disk test is used to measure the coefficient of friction of the selected materials in different conditions and with different parameters. The parameters are selected to mimic the conditions of the applications in real life as well as possible to get relevant information of the material. The polymer material is tested against steel as the sliding couple in the real application is also steel.

The pin-on-disk device used in the measurements is UMT-2 Pin/Ball-on-disk equipment by CETR, a picture of the device is seen in Figure 10. The equipment fulfils an ASTM G99 -95a standard. With an elevated-temperature chamber the temperature range achieved is from -20 °C to +350 °C. However, the heating unit of the device was broken, therefore the tests were conducted only in around room temperature. The revolve disk speed range is 0,1 – 1000 rpm. The used disk size was 65 mm and pin size 10 mm. The pin was placed 25 mm from the center of the disk.

Figure 10. CETR UMT-2 Pin/Ball-on-disk equipment.

4.3.1 Sample preparation for pin-on-disk

In the pin-on-disk measurement, the sample holder is 10 mm in diameter and the depth of the holder is 7 mm. Therefore, the sample dimensions are 10 mm in diameter and approximately 9 mm in height. The UTEC6540 was first flattened to 9 mm thickness and then specimens with a diameter of 10 mm were drilled from the material with a pilar drilling machine. The PE1000R and Tivar materials were first cut to thickness of 9 mm and the specimens were drilled from the slice. Six to eight parallel samples were prepared from each plastic type. The pictures of the specimen are presented in Figure 11.

A sample from the Vespel integrated slider was supposed to be drilled in a way which incorporated both UHMWPE and Vespel in the same sample, but unfortunately the method did not work for Vespel integrated slider, because the Vespel part disintegrated from the bulk material. It would have been interesting to test the actual Vespel integrated slider to understand the friction forces in a real part. Instead, pure Vespel material sourced by the company was tested. The Vespel part was a rod with a diameter of 20 mm and length of 200 mm. The original rod was machined into a rod with a diameter of 10 mm and a length of about 40 mm. Three samples with a length of approximately 9 mm were cut from it with a circular saw and the surface was grinded to get a smooth surface. The pictures of the specimen are presented in Figure 11.

Figure 11. Pin-on-Disk samples of UTEC6540, PE1000R, Tivar and Vespel, from left to right.

The steel type used in the application was 4030 with a Rockwell hardness of 33. The steel disk for the measurements was selected to correspond the actual application as well as possible to the steel in. The disk was changed to a new one with every material. A picture of the disk is presented in Figure 12.

Figure 12. A steel disk with a diameter of 65 mm.

4.3.2 Measurement procedure for pin-on-disk

The aim of the test was to measure the COF in different temperatures (-40°C to 23°C). The oven attached to the pin-on-disk device was out of operation, thus the measurements were done in isothermal conditions in ambient room temperature and the effect of changing the speed and pressure was studied. In addition, the cooling unit tested whether lower temperatures could be achieved. However, the temperature of the cool air

could not be controlled due to the broken oven, instead the system could cool down to the minimum temperature of about -20 °C but the temperature could not be kept constant because the pressure of the dryer system increased too much probably due to accumulated moisture and ice.

The anticipated vehicle application defined the pressure applied on the steel track clips. The pressure was calculated by using the mass of the vehicle including two passengers. The pressure on a flat surface was estimated to be 0,16847 MPa, which would be the lowest applied pressure. The highest pressure was estimated when ¼ of the track clips are in contact. This would happen for instance if driven over a bump in reality. The highest applied pressure was estimated to be 0,67388 MPa.

The contact force can be calculated with the following equation:

$$F = p \times A_{pin} \quad (8)$$

Where *p* is the applied pressure and *A* is contact area.

The contact area of the pin with a diameter of 10 mm is calculated by using the following formula:

$$A_{pin} = r^2\pi \quad (9)$$

$$A_{pin} = (5mm)^2\pi = 78{,}5\ mm^2$$

The maximum and minimum forces are calculated by using the equation 8:

$$F_{min} = 0{,}16847\ MPa \times 78{,}5mm^2 = 13{,}2249\ N$$

$$F_{max} = 0{,}67388\ MPa \times 78{,}5mm^2 = 50{,}87794\ N$$

The parameters selected for the load were 20 N, 37 N and 54 N, which would correspond the forces in the real-life application. The minimum load of 20 N was selected, because with lower loadings (12 N) the noise, i.e., the sinusoidal fluctuation of the friction force was significantly higher compared to loadings above 20 N.

The estimated velocity of the vehicle is approximately 25 – 50 km/h. The maximum velocity of the pin-on-disk device was 1000 rpm, which corresponds to approximately 9,4 km/h with a 25 mm radius of the pin from the center of the disk. Due to the fact the device could not reach such high velocities as in the application, the test parameters for the velocity do not correspond to the real-life application. The selected velocities were 60 rpm, which corresponds to 0,56 km/h, 300 rpm (2,82 km/h) and 600 rpm (5,64 km/h). Higher velocities were not used, because even the 600 rpm caused some resonance which loosened the screws of the sample holder causing the sample holder to detach from the device, so longer tests with higher velocities were not performed.

The steel disk for the measurements was selected to correspond as well as possible to the steel in the actual application. The diameter of the disk was 65 mm. The disk was changed to a new one for every material tested. The sample holder of the pin was 10 mm in diameter. A picture of the sample holder is presented in Figure 13.

Figure 13. Sample holder with a sample cavity diameter of 10 mm.

The parameters used in the measurements are presented in Table 6. The tests were planned so, that when a new sample was changed, first a longer test (60 or 90 minutes) was done to “wear in” the sample. This way the effect of unregular surface roughness was minimized. After the longer test, a ramp test, with different loadings was performed with various velocities. In between the ramp test the fastening of the sample was checked to prevent the sample from loosening. Two parallel measurements were done for the candidate materials.

Table 6. Parameters of pin-on-disk measurements with dry contact.

Test	Sequence	Duration (min)	Force (N)	Velocity (rpm)
Long	1	90 or 60	54	300
Ramp 1	1	2	20	60
	2	2	37	60
	3	2	54	60
	4	2	20	60
Ramp 2	1	2	20	300
	2	2	37	300
	3	2	54	300
	4	2	20	300
Ramp 3	1	2	20	600
	2	2	37	600
	3	2	54	600
	4	2	20	600

Special lubricant tests were done so, that first a reference test with 30 minutes and 60rpm was conducted, after which a test with 14 mL of water lubricant and with the same parameters (30 minutes and 60 rpm) was conducted. The volume of 14 mL of water could cover the whole surface of the disk. The speed of 60 rpm was selected, because at higher speeds the water would start to escape to the sides of the measurement vessel and the pin wouldn't stay in wet contact the whole duration of the test. The parameters of lubricated tests are presented in Table 7.

Table 7. Parameters of pin-on-disk measurement with lubricant.

Test	Duration (min)	Force (N)	Velocity (rpm)	Lubricant
Dry	30	54	60	-
Lubricated	30	54	60	Water 14 mL

5. RESULTS AND ANALYSIS

5.1 Tensile testing results

In Figure 14, Figure 15, Figure 16, and Figure 17, the stress-strain curves for each material studied in this thesis are presented. In general, the results of the tensile tests are rather coherent between the parallel specimens. The results of UTEC6540 samples, in Figure 14, show relatively stiff and brittle behaviour compared to PE1000R (see Figure 15) and Tivar (see Figure 16) materials, where the strain hardening effect is more dominant. The elastic region of the curves for UTEC6540, PE1000R and Tivar are similar including the yield point. For Vespel material (see Figure 17) the stress-strain curve is completely different compared to the other materials. Vespel specimens indicate very high strength and low strain to break compared to other materials.

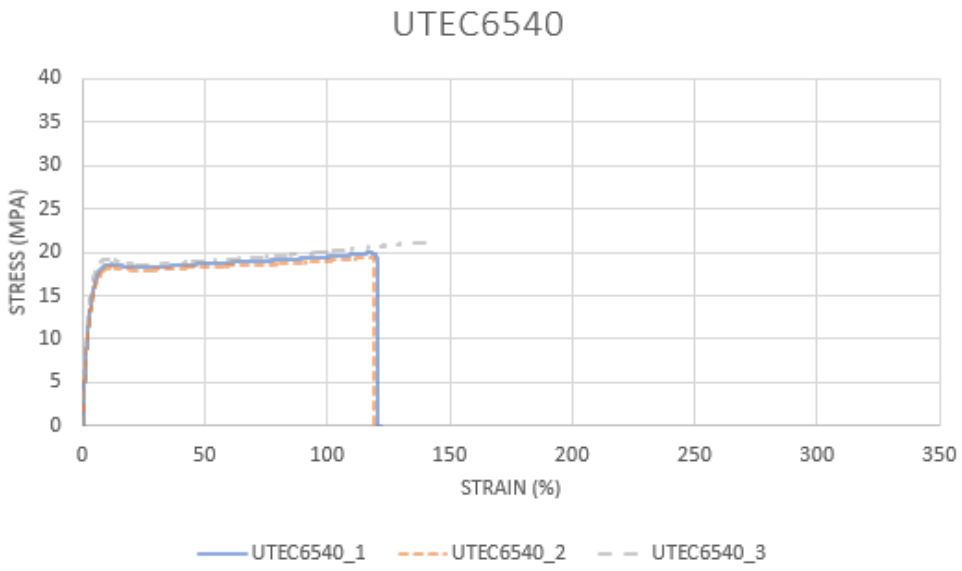

Figure 14. Tensile test results of UTEC6540 with displacement rate of 5mm/min.

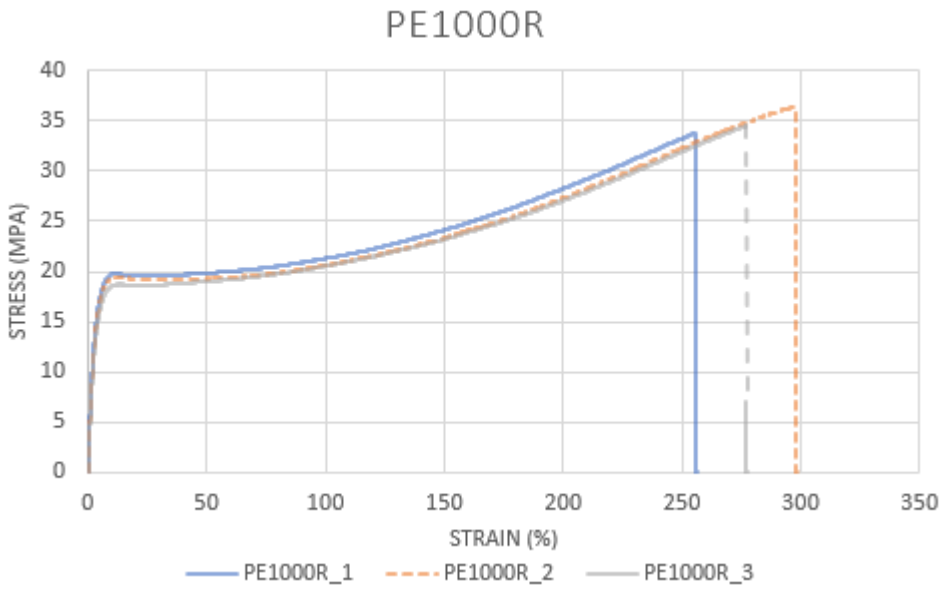

Figure 15. Tensile test results of PE1000R with displacement rate of 5mm/min.

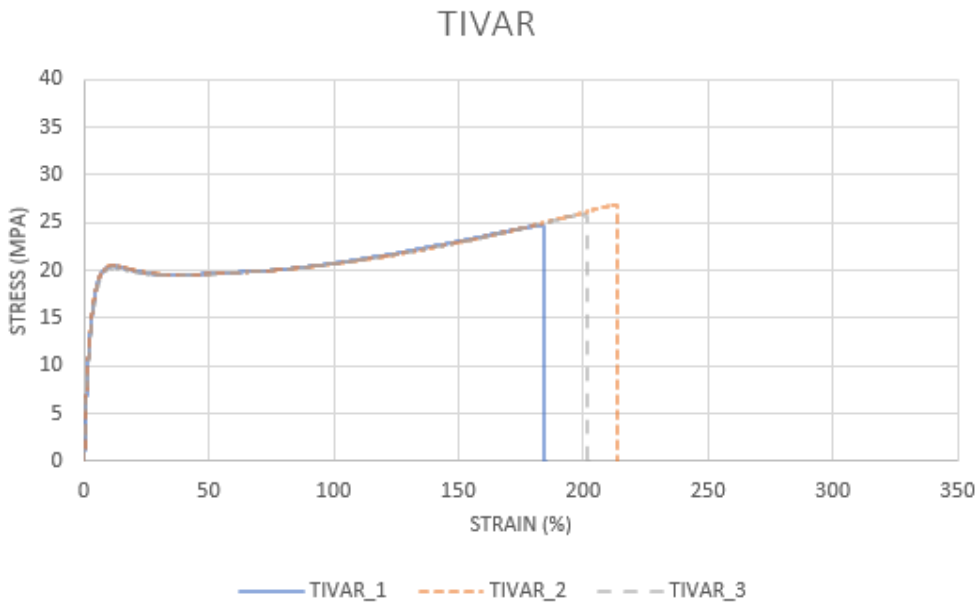

Figure 16. Tensile test results of Tivar with displacement rate of 5mm/min.

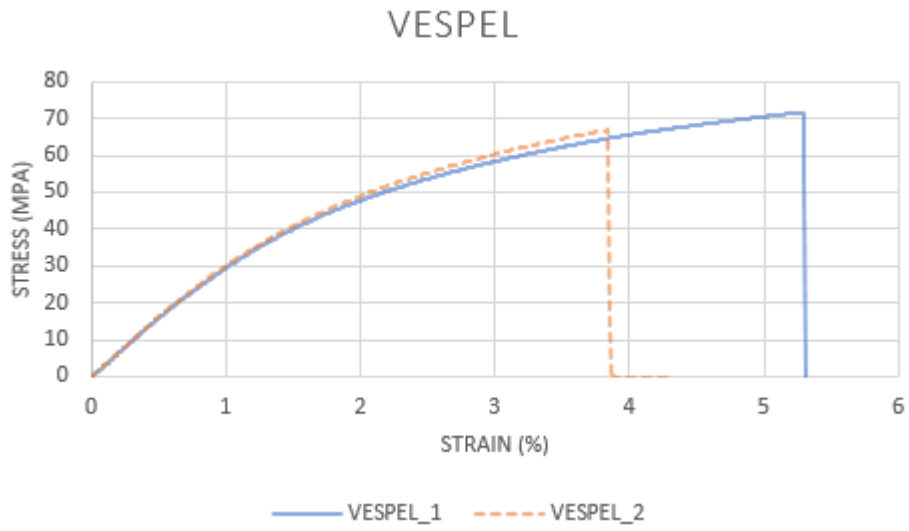

Figure 17. Tensile test results of Vespel with displacement rate of 5mm/min.

In Figure 18, the stress-strain curves of the UHMWPE tests are compared (specimens of UTEC6540, PE1000R and Tivar). Looking at the shape of the stress-strain curves, the shape is essentially similar with these materials regarding the elastic region and yield point. PE1000R shows the largest strain hardening effect and UTEC6540 indicate the least strain hardening. Strain hardening is related to a higher degree of crystallization if material breaks at a higher stress level compared to yield point.

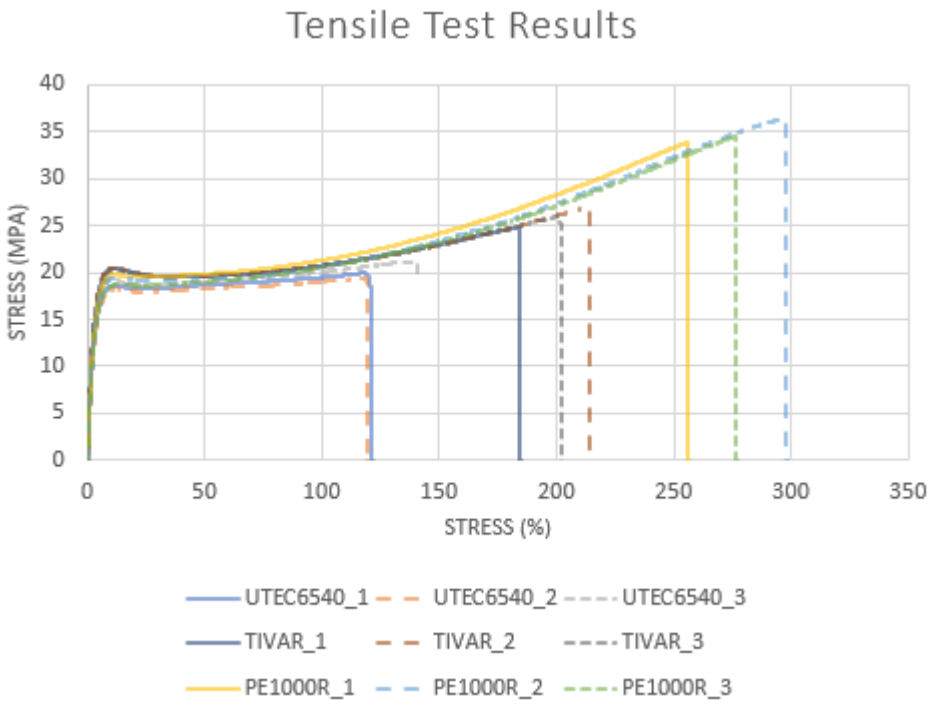

Figure 18. Comparison of tensile test results of all the UHMWPE specimens (UTEC6540, PE1000R and Tivar).

In Table 8, the average tensile properties of the materials are presented. As seen in Table 8, the Young's modulus of UTEC6540, PE1000R and Tivar are similar with each other. Compared to UTEC6540, the modulus of PE1000R is 6,8 % lower compared to UTEC6540. The Young's modulus on Tivar is 5,2% higher than that of UTEC6540. The ultimate tensile strength has more variation between series; UTEC6540 has the lowest tensile strength (20,15 MPa). PE1000R has 73,4 % higher strength than UTEC6540. Tivar has 28,2 % higher tensile strength compared to UTEC6540. When comparing the ultimate elongation, UTEC6540 has the lowest elongation to break (122,1 %). When compared to UTEC6540, Tivar has 61,9 % higher elongation to break compared to UTEC6540. An PE1000R has 126% higher elongation to break compared to UTEC6540.

At the yield point, the elongation values are very similar with UTEC6540, PE1000R and Tivar samples, as seen in Table 8. UTEC6540 shows the lowest yield strength, PE1000R has 5,3 % higher yield strength compared to UTEC6540. Tivar has 11,2 % higher yield point compared to UTEC6540. The elongation at yield point is lowest for UTEC6540, and PE1000R has 6,1 % higher elongation at yield compared to UTEC6540. Tivar has 20,2 % higher elongation at yield compared to UTEC6540.

Vespel has significantly higher Young's modulus compared to the other materials, about 5,6 times higher compared to UTEC6540 (see Table 8). In addition, the tensile strength for Vespel is 3,4 times higher compared to UTEC6540. However, the elongation at break for Vespel is only 4,5 %, which is 96 % less compared to UTEC6540.

Table 8. Average values of tensile test results.

Property	UTEC6540	PE1000R	TIVAR	VESPEL
Young's modulus (MPa)	553,1	515,5	581,8	3109
Yield strength (MPa)	18,29	19,26	20,33	-
Tensile strength (MPa)	20,15	34,95	25,84	69,10
Elongation at break (%)	122,1	275,8	197,7	4,532
Elongation at yield (%)	10,91	11,58	13,11	-

In Figure 19, Figure 20, and Figure 21, the pictures of the different phases phases of material behaviour during tensile loading are presented. First, there is the initial stage. Second, there is the sample during the test before breaking. The third phase is taken after the breakage of the specimen. The test with Vespel was so fast (the behavior occurred fast at the applied displacement rate), that no pictures were taken of the process.

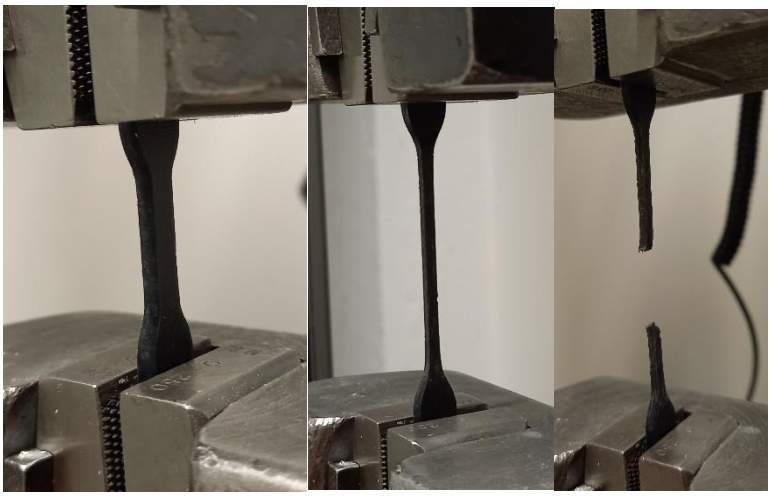

Figure 19. Tensile testing of UTEC6540: initial phase, elongation and breakage.

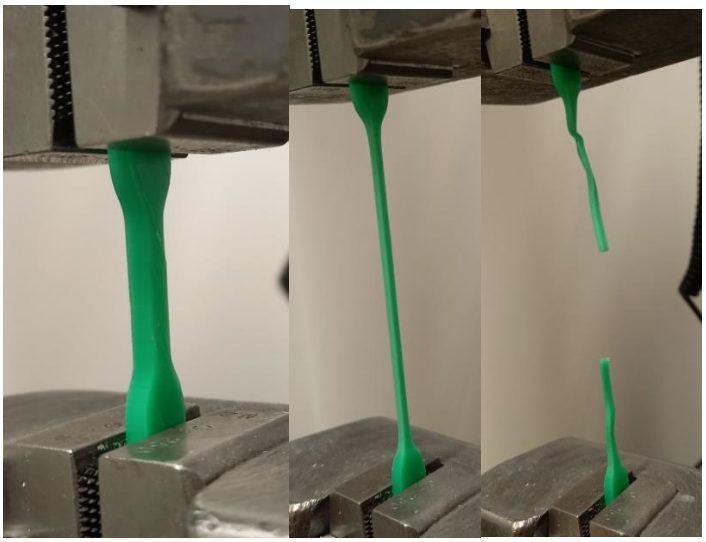

Figure 20. Tensile testing of PE1000R: initial phase, elongation and breakage.

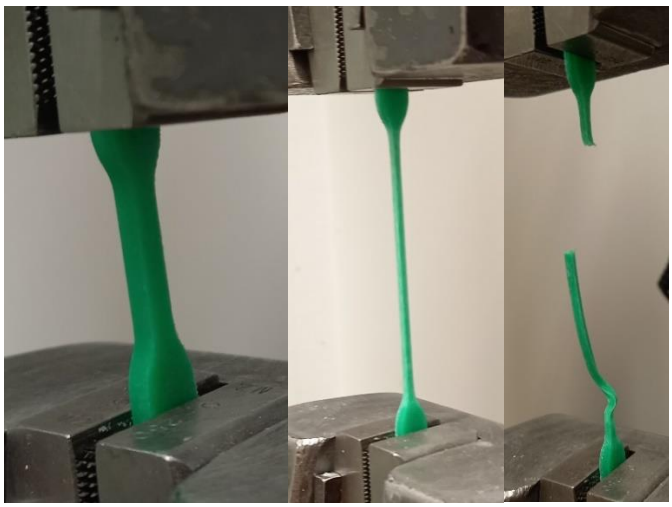

Figure 21. Tensile testing of Tivar: initial phase, elongation and breakage.

In Figure 22, Figure 23, Figure 24, and Figure 25, specimens per series are shown as they appear after the tests. All the specimens broke at the gauge section of the specimen geometry.

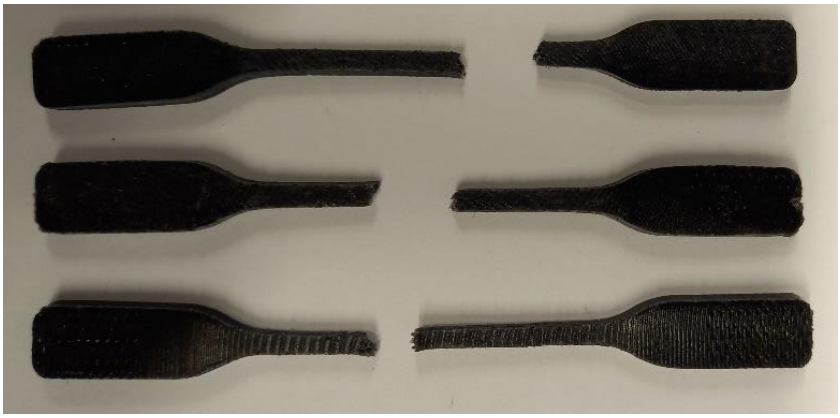

Figure 22. Tensile test specimens of UTEC6540 after the testing.

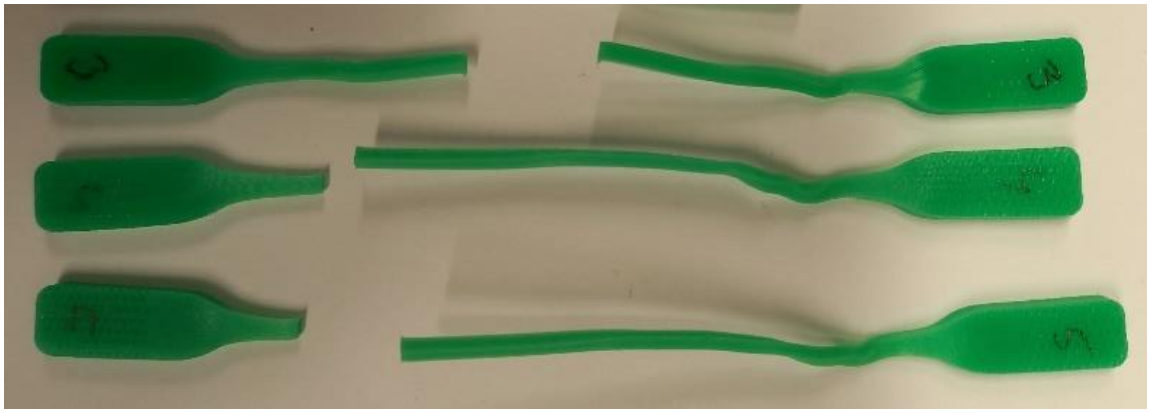

Figure 23. Tensile test specimens of PE1000R after the testing.

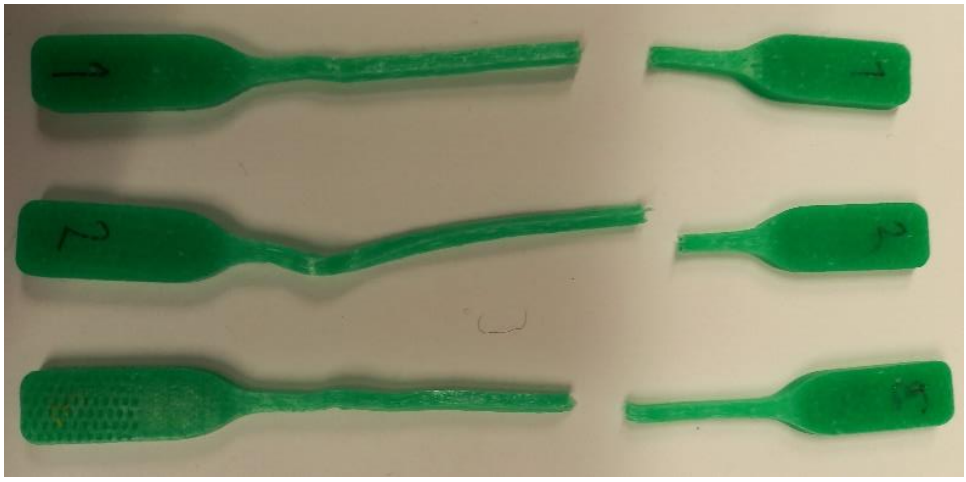

Figure 24. Tensile test specimens Tivar after the testing.

Figure 25. Tensile test specimens of Vespel after the testing.

5.2 DMA results

The results of the pre-test for UTEC6540 are shown in Figure 26, Figure 27, and Figure 28. In Figure 26, the results of force offset (FO) test are presented. The force segment with the highest Young's modulus is the force offset value. The highest value for the modulus is reached at segment 8, which corresponds to a force of 16 N.

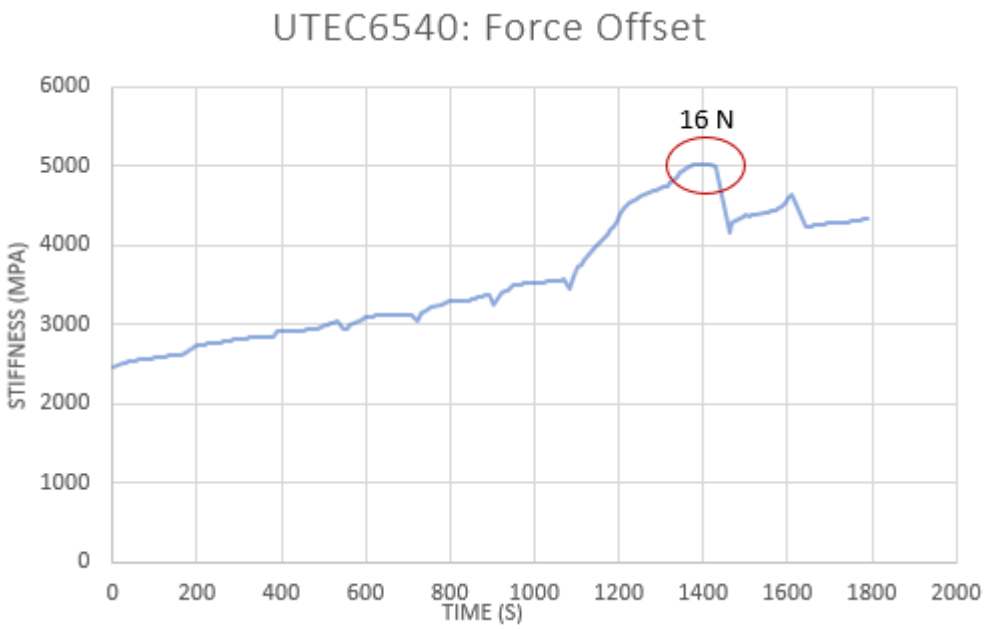

Figure 26. Results of force offset (FO) for UTEC6540 sample.

The results of the pre-tests for Displacement Amplitude (DA) are presented in Figure 27 and results for Force Amplitude (FA) are presented in Figure 28. The displacement amplitude for further tests is selected as the point from where the linear region of the curve ends.

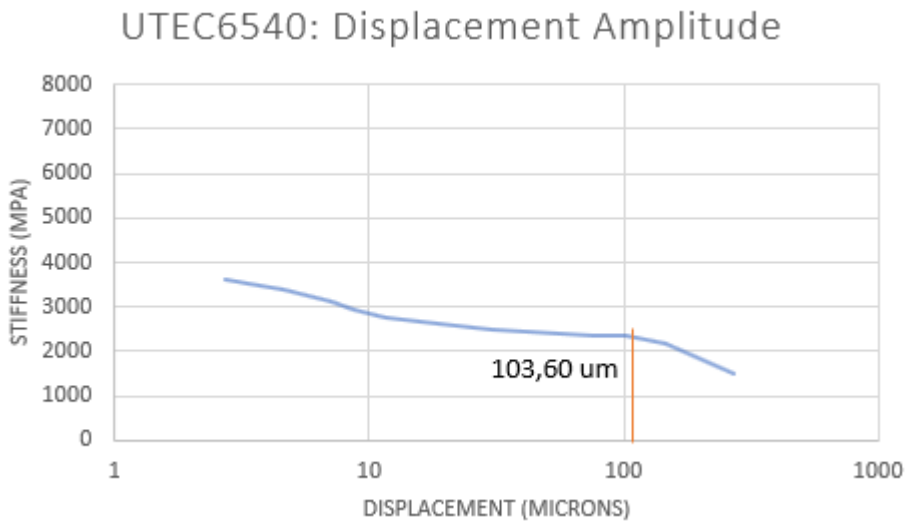

Figure 27. Results of displacement amplitude (DA) for UTEC6540.

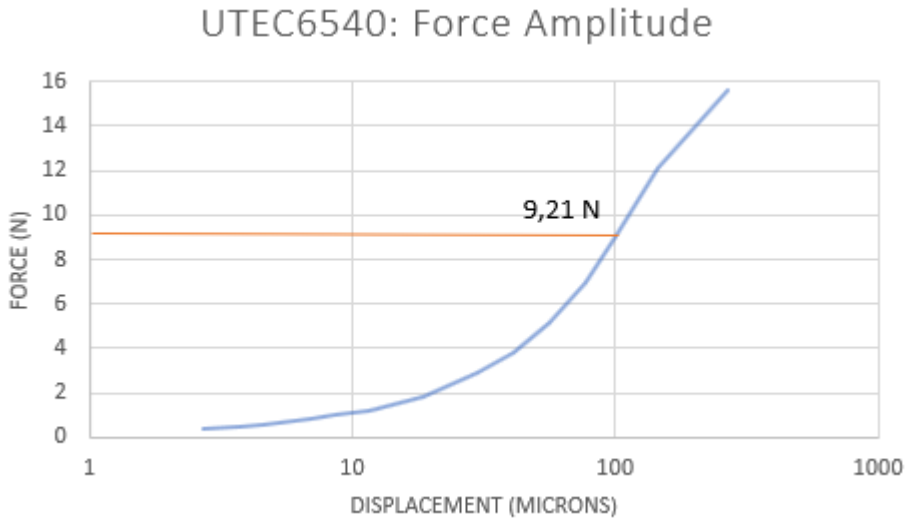

Figure 28. Results for force amplitude (FA) for UTEC6540.

The pre-test for the PE1000R, Tivar and Vespel samples are done similarly, and the results of these tests can be found in Appendix 1. The results of the pre-tests are presented in Table 9.

Table 9. Results of DMA pre-tests.

Parameter	UTEC6540	PE1000R	TIVAR	VESPEL
Force Offset (N)	16	14	18	19
Force Amplitude (N)	9,21	6,55	9,29	7,98
Displacement Amplitude (µm)	103,60	100	100	40

The actual tests were done over a temperature range of -55 Cº to +120 Cº and by using a frequency of 10 Hz. In Figure 29, Figure 30, Figure 31, and Figure 32, the results of DMA measurement for all the material series are presented.

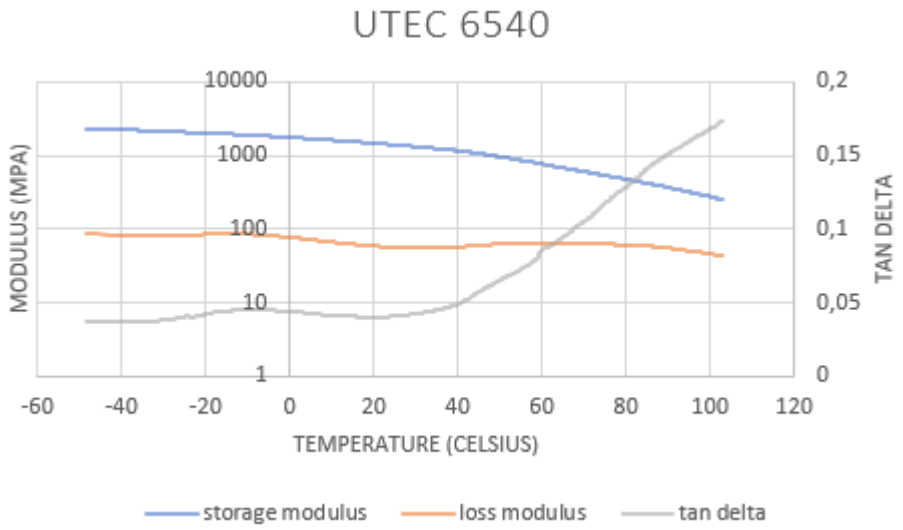

Figure 29. Storage modulus (G'), loss modulus and tan δ results of UTEC6540 with 10 Hz frequency and temperature sweep from -55 Cº to +120 Cº.

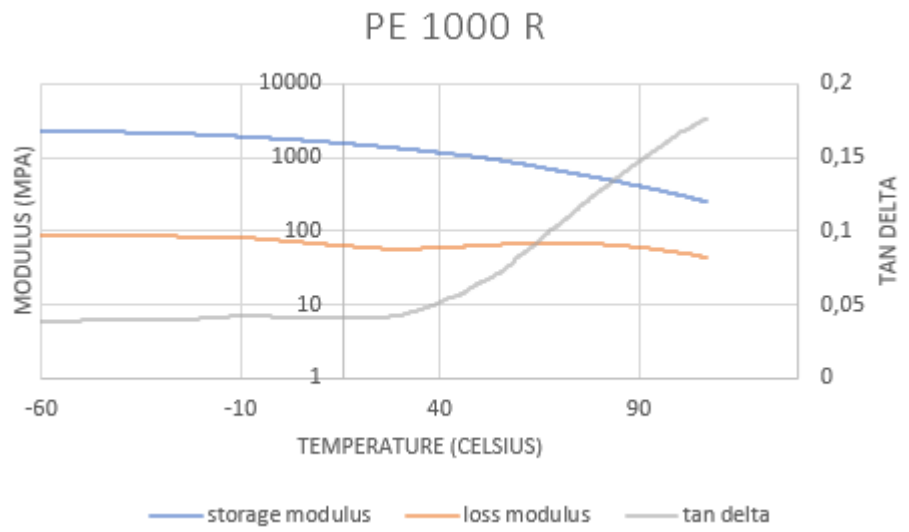

Figure 30. Storage modulus (G'), loss modulus and tan δ results of PE1000R with 10 Hz frequency and temperature sweep from -55 C° to +120 C°.

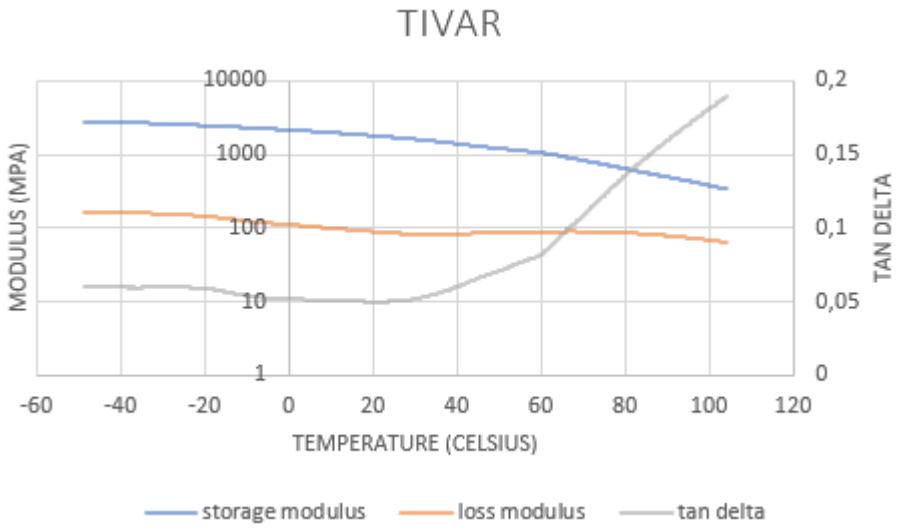

Figure 31. Storage modulus (G'), loss modulus and tan δ results of Tivar with 10 Hz frequency and temperature sweep from -55 C° to +120 C°.

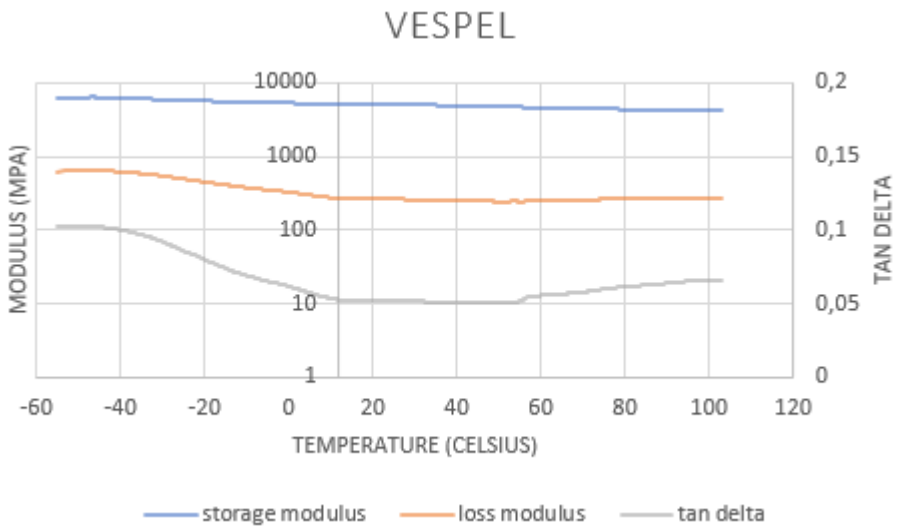

Figure 32. Storage modulus (G'), loss modulus and tan δ results of Vespel with 10 Hz frequency and temperature sweep from -55 C° to +120 C°.

In Figure 33, the comparison of the DMA tests results for storage modulus are presented. All the series show a rather constant storage modulus. The storage modulus of samples made from UHMWPE (UTEC6540, PE1000R and Tivar) starts to decrease above around +60 ºC. The maximum operating temperature of UHMWPE is +80 ºC (Wefapress, 2020). Thus, the storage modulus results of DMA measurement correlate with the current literature. From Figure 33 it can be seen, that UTEC6540 and PE1000R samples have very similar behaviour. Tivar series has slightly higher (20 % higher compared to UTEC6540) storage modulus at lower temperatures compared to UTEC6540 and PE1000R. The Vespel series has much higher storage modulus than the other UHMWPE series. The storage modulus of Vespel is 2,7 … 3,5 times higher compared to UTEC6540. In Table 10 and Figure 34, the results are presented for selected temperatures of -40 ºC, -25 ºC, 0 ºC, and +25 ºC. When comparing the candidate materials (PE1000R, Tivar and Vespel) to the rival material UTEC6540 it can be seen from Figure 34, that PE1000R has very similar storage modulus compared to UTEC6540, and Tivar has approximately 20 % higher storage modulus compared to the rival, and Vespel has clearly higher storage modulus compared to the rival. In conclusion, Vespel material has the highest storage modulus i.e., stiffness across the temperature range of -55 ºC to +120 ºC.

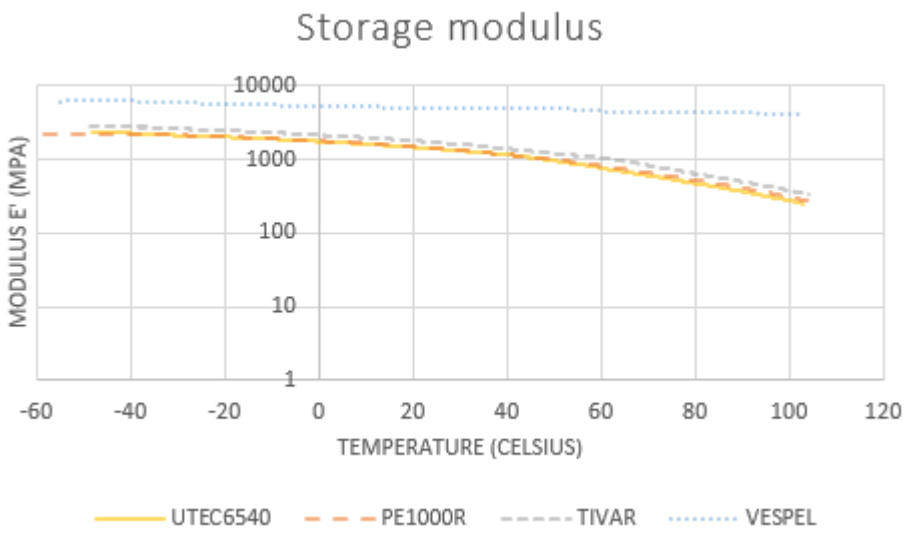

Figure 33. Comparison of storage modulus (G').

Table 10. Storage modulus results of the series in selected temperatures (-40 °C, -25 °C, 0 °C, and +25 °C).

Series	-40 °C	-25 °C	0 °C	+25 °C
UTEC6540 (MPa)	2256	2057	1748	1384
PE1000R (MPa)	2193	2095	1779	1401
TIVAR (MPa)	2777	2524	2141	1695
VESPEL (MPa)	6174	5769	5273	4998

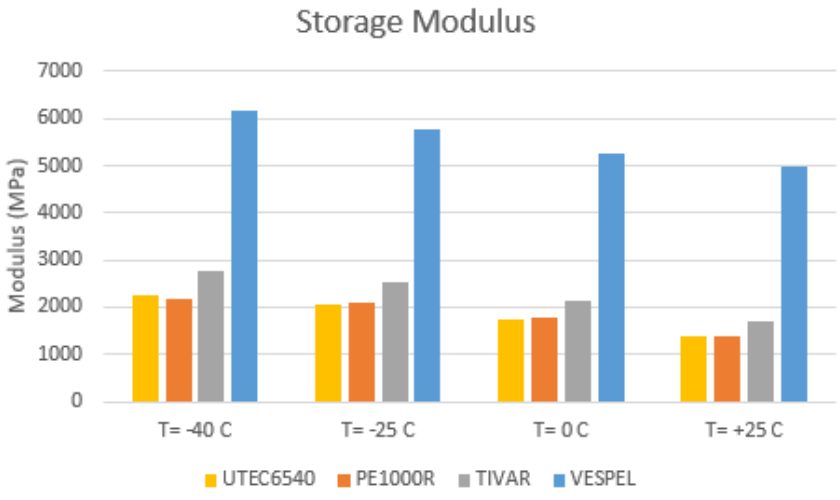

Figure 34. Comparison of storage modulus values of test series at different temperatures (-40 °C, -25 °C, 0 °C, and +25 °C).

In Figure 35, the results of the loss modulus of the series are compared. From Figure 35 it can be seen, that there are no peaks in the loss modulus graphs indicating there is no

major irreversible changes in the samples. In Table 11 and in Figure 36, the loss modulus values are presented for selected temperatures (-40 ºC, -25 ºC, 0 ºC, and +25 ºC). From these figures (see Figure 35 and Figure 36) it can be seen, that PE1000R series has very similar loss modulus profile compared to the reference UTEC6540 series. Tivar series has 1,4 to 2 times higher loss modulus compared to UTEC6540. Vespel series has very different loss modulus profile compared to the other series. At low temperatures (-40 ºC and -25 ºC) Vespel has 7,4 to 5,9 times higher loss modulus compared to UTEC6540. At temperatures above 0 ºC the loss modulus is 4,3 to 4,6 times higher compared to UTEC6540. This indicates higher heat generation for Vespel during dynamic loading. However, the tan δ curve has a similar trend with other series.

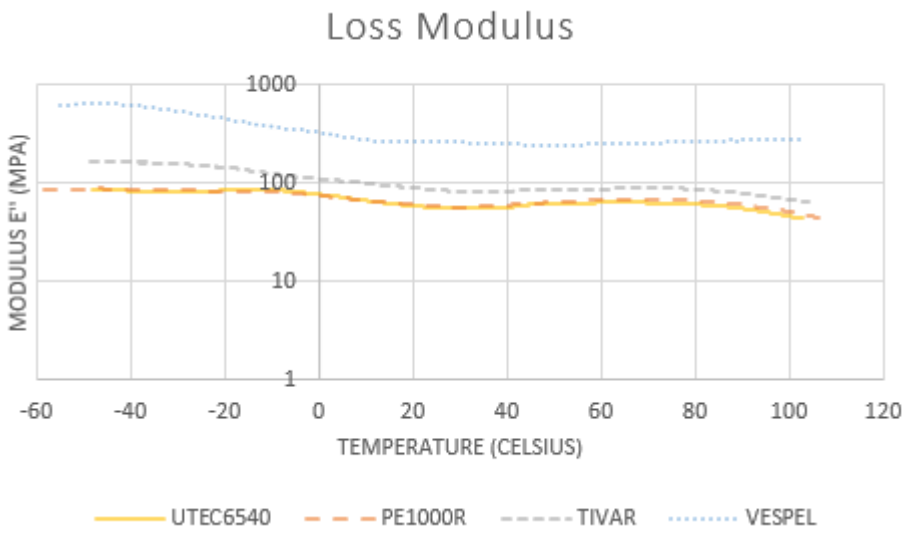

Figure 35. Comparison of loss modulus (G'')

Table 11. Loss modulus results of the series in selected temperatures (-40 ºC, -25 ºC, 0 ºC, and +25 ºC).

Series	-40 ºC	-25 ºC	0 ºC	+25 ºC
UTEC6540 (MPa)	84	84	76,96	57
PE1000R (MPa)	87	84	74	58
TIVAR (MPa)	166	152	112	85
VESPEL (MPa)	618	493	327	262

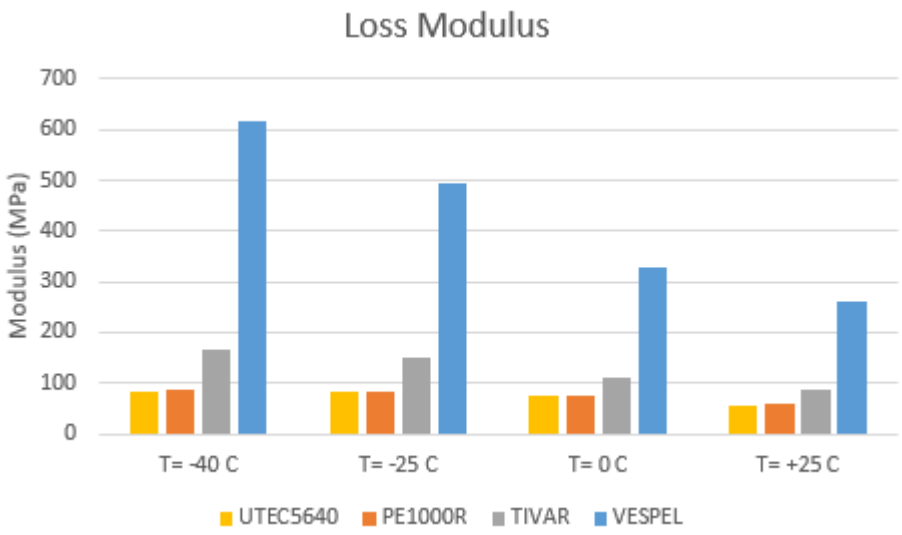

Figure 36. Comparison of loss modulus values of test series at different temperatures (-40 ºC, -25 ºC, 0 ºC, and +25 ºC).

In Figure 37, the comparison of tan δ graphs is presented for every series. In Table 12 and Figure 38, the tan δ results are presented for the selected temperatures (-40 ºC, -25 ºC, 0 ºC, and +25 ºC). From Figure 37 it can be seen, that UTEC6540, PE1000R and Tivar samples follow approximately the same curve: tan δ value starts to increase at about +40 ºC. Tan δ corresponds to the ratio of E'' and E'. The increase in tan δ could indicate a phase change. The curve of Vespel series is different from the other tan δ graphs showing only slight increase in tan δ at +50 ºC and clear increase below 0 ºC. When comparing the tan δ values at the selected temperatures (see Table 12 and Figure 38), it can be seen that, again, PE1000R has similar values compared to UTEC6540 series. The Tivar series has 1,2 to 1,6 times higher tan δ values compared to UTEC6540. The Vespel series has 2,7 to 1,3 times higher tan δ values compared to UTEC6540 at the selected temperatures. However, above +25 ºC, the tan δ values of UHMWPE series start to increase, whereas the tan δ values of Vespel remain rather constant.

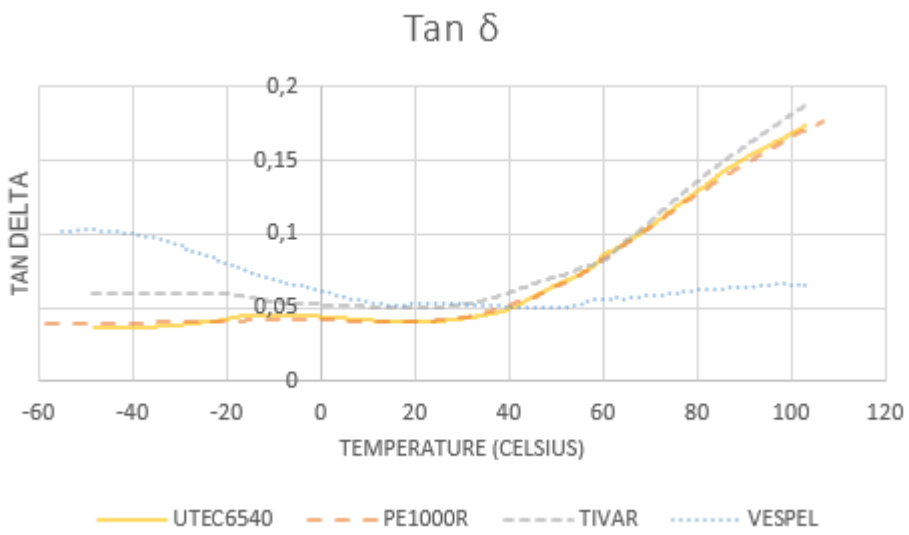

Figure 37. Comparison of tan δ values of the different test series.

Table 12. Tan delta results of the test series at selected temperatures (-40 °C, -25 °C, 0 °C, and +25 °C).

Series	-40 °C	-25 °C	0 °C	+25 °C
UTEC6540	0,04	0,04	0,04	0,04
PE1000R	0,04	0,04	0,04	0,04
TIVAR	0,06	0,06	0,05	0,05
VESPEL	0,10	0,09	0,06	0,05

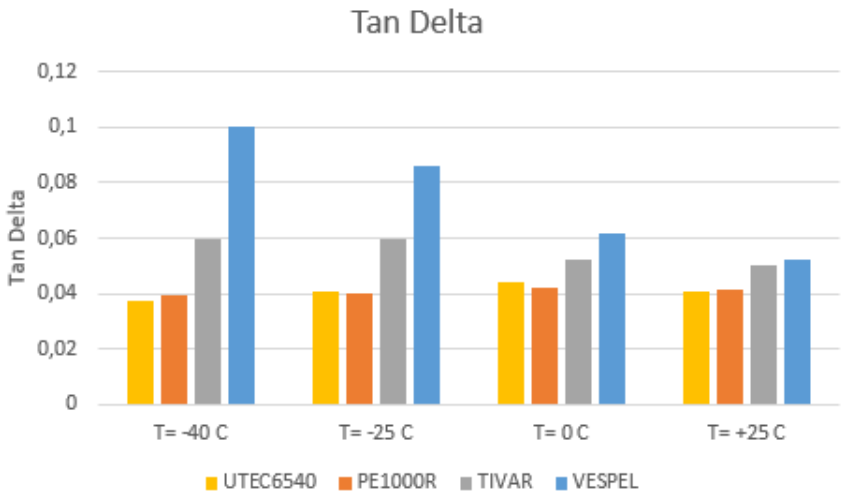

Figure 38. Comparison of tan δ values of test series at different temperatures (-40 °C, -25 °C, 0 °C, and +25 °C).

5.3 Pin-on-Disk test results

5.3.1 Dry contact surface

In dry contact surface tests, generally one longer test was first done with a sample, after which a ramp test with different speeds and loadings was performed with the same sample. This was done to “run in” the sample, so the results of the ramp tests would be more representative. Then, the results in the thesis can be better compared.

In Figure 39, Figure 40, Figure 41, and Figure 42, the results of the long tests of the different test series are presented. The tests were done with a speed of 300 rpm and with a load of 54 N. The duration of the tests are 60 or 90 minutes. First, the long tests were done with the duration or 90 minutes but, if the COF values remain constant during the test, the duration of the long test was decreased to 60 minutes.

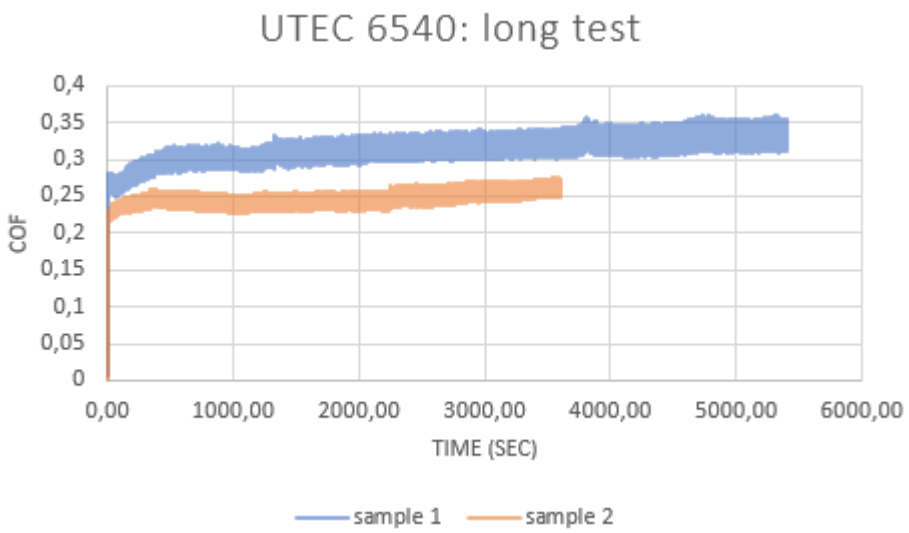

Figure 39. Results of UTEC6540 series sample 1 and 2 in a long test with 54 N force and 300 rpm speed.

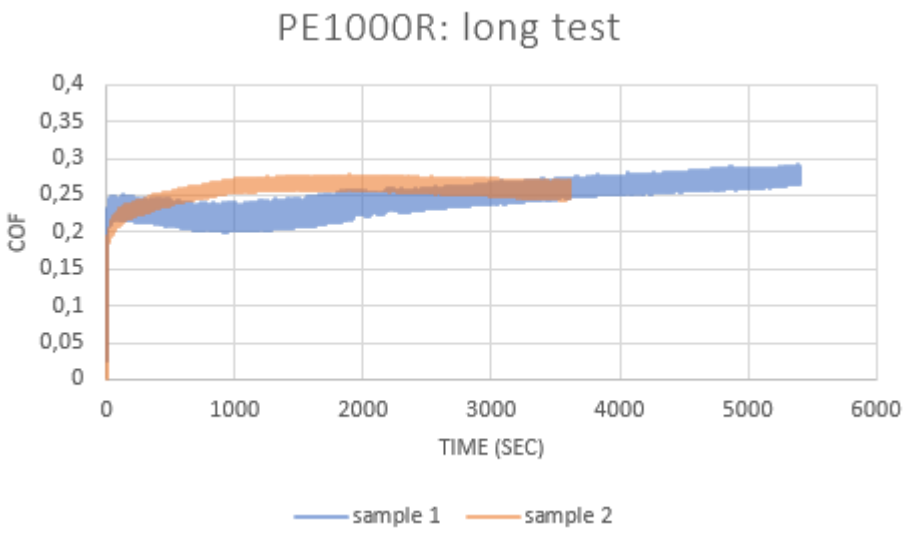

Figure 40. Results of PE1000R series samples 1 and 2 in a long test with 54 N force and 300 rpm speed.

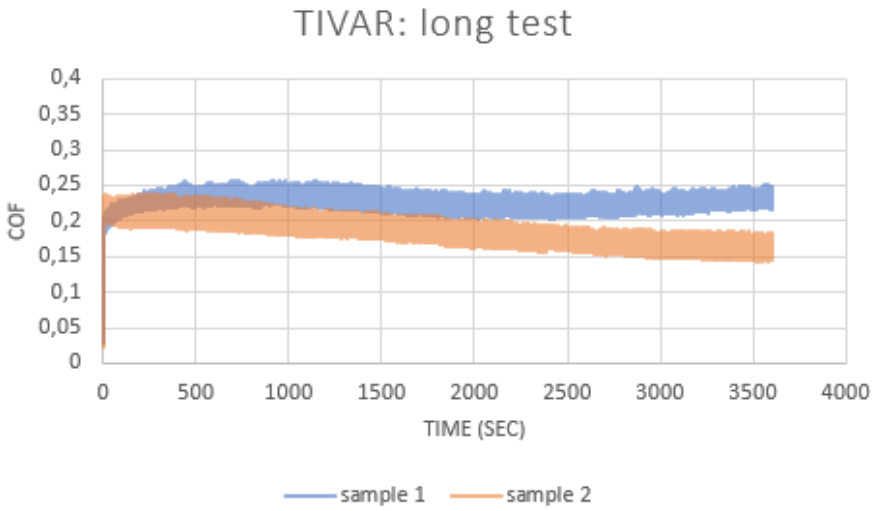

Figure 41. Results of TIivar series samples 1 and 2 in a 60-minute test with 54 N force and 300 rpm speed.

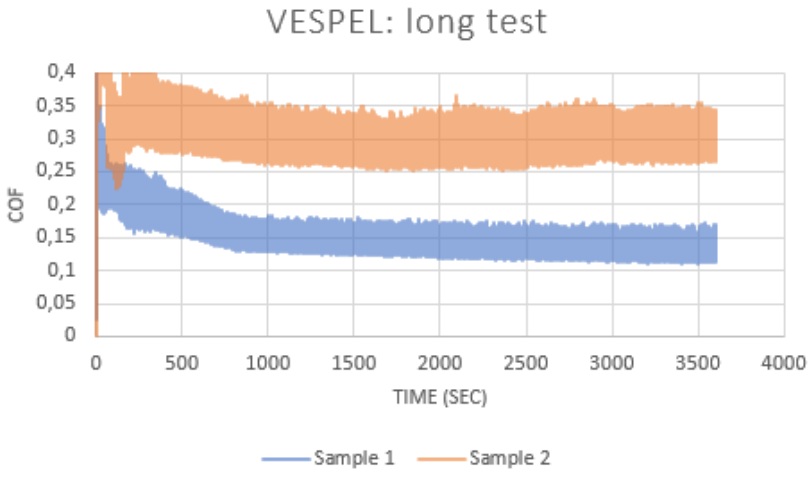

Figure 42. Results of Vespel series samples in a 60-minute test with 54 N force.

In Table 13 and Figure 43, the average COF values for each series and sample are presented. As seen in Table 13, UTEC6540 has the highest COF in average (0,275). The lowest average COF is found for Tivar (0,21), which is 24 % less than average COF of UTEC6540. Vespel has on average the second lowest average COF (0,23), which is 16 % less compared to UTEC6540. PE1000R has a slightly lower average COF (0,255), which is 7,3 % lower compared to UTEC6540.

Table 13. Average COF values of long tests.

Series	Sample 1	Sample 2	Average COF	Comparison of average COF to UTEC6540 (%)
UTEC6540	0,31	0,24	0,275	100
PE1000R	0,25	0,26	0,255	92,7
TIVAR	0,23	0,19	0,21	76,4
VESPEL	0,15	0,31	0,23	83,6

The differences between COF values of the different samples and series vary significantly. As seen in Figure 43, the largest difference between two tested samples is with Vespel material, where sample 1 has 52 % lower COF compared to sample 2. The average COF in the ramp test for Vespel is 0,35 with 54 N force and 300 rpm speed (see Table 19). This could indicate that the result for Vespel sample 2 represents more the average COF. The difference between two test samples for UTEC6540 is 23 %, with Tivar samples 21 % and with PE1000R samples 3,9 %. To get more reliable results, more parallel samples should have been used. Especially with Vespel samples, the difference of average COF between the samples is very large. The lower COF value is the lowest among the series, and the higher COF value is the highest among the series. In conclusion, the recycled materials PE1000R and Tivar seem to have lower COF compared to the original UTEC6540 material. The case of Vespel, the average COF from the long tests indicate that COF could be lower compared to UTEC6540.

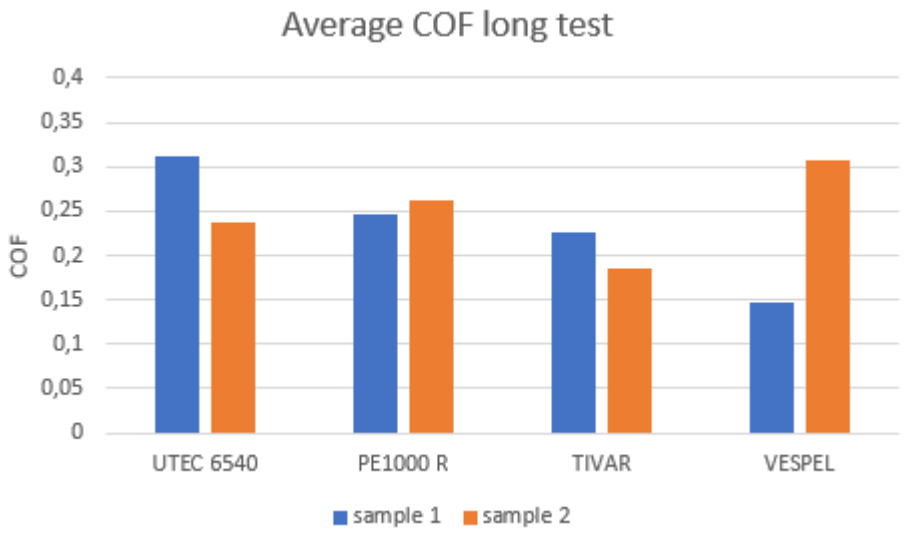

Figure 43. Average COF values of different materials in the long pin-on-disk tests.

In Figure 44 and Figure 45, Figure 46, Figure 47, Figure 48, and Figure 49, the results of the ramp tests are presented. The ramp test was done with three different speeds: 60 rpm, 300 rpm and 600 rpm. First 2 minutes (120 seconds) of testing is done with 20 N loading, then, 2-4 minutes (120-280 seconds) are done with 37 N loading, and, third, 4-6 minutes (280-360 seconds) are done with 54 N loading. The last loading period of 6-8 minutes (360-480 seconds) is tested with 20 N loading to see if there are any changes to the friction between the beginning and the end of the test (return to the same loading).

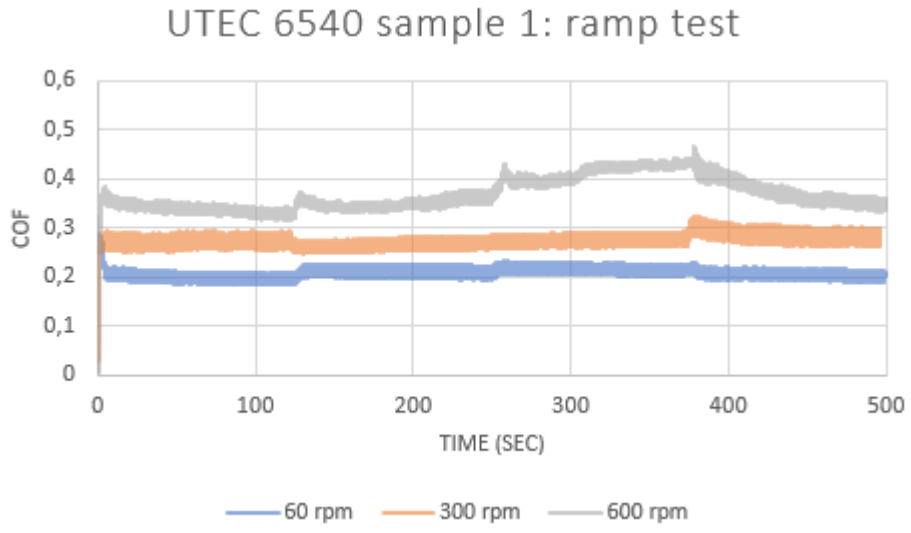

Figure 44. UTEC6540 sample 1 ramp test with different loadings (20 N, 37 N, 54 N and 20 N) and with different speeds (60 rpm, 300 rpm and 600 rpm).

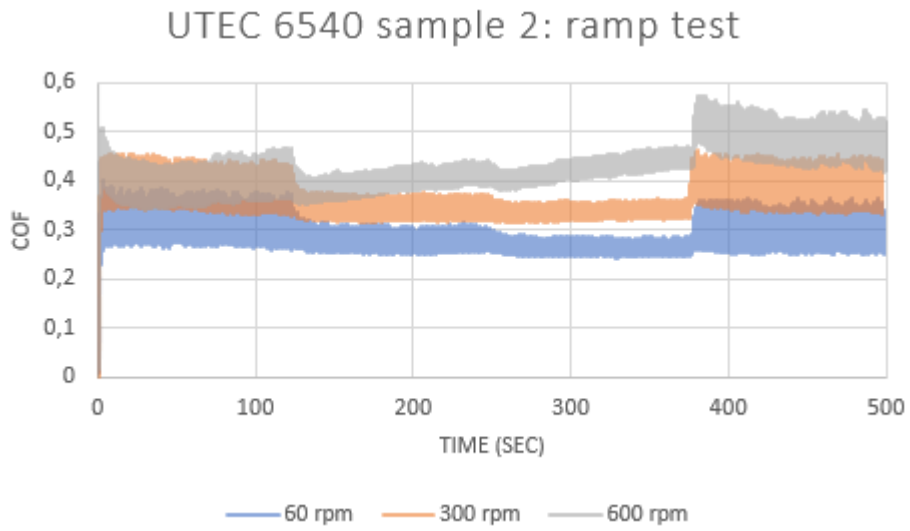

Figure 45. UTEC6540 sample 2 ramp test with different loadings (20 N, 37 N, 54 N and 20 N) and with different speeds (60 rpm, 300 rpm and 600 rpm).

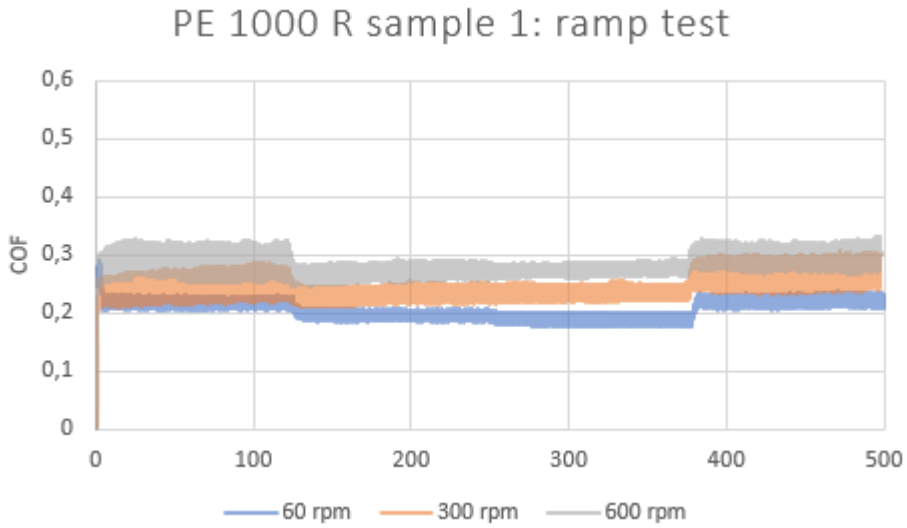

Figure 46. PE 1000 R sample 1 ramp test with different loadings (20 N, 37 N, 54 N and 20 N) and with different speeds (60 rpm, 300 rpm and 600 rpm).

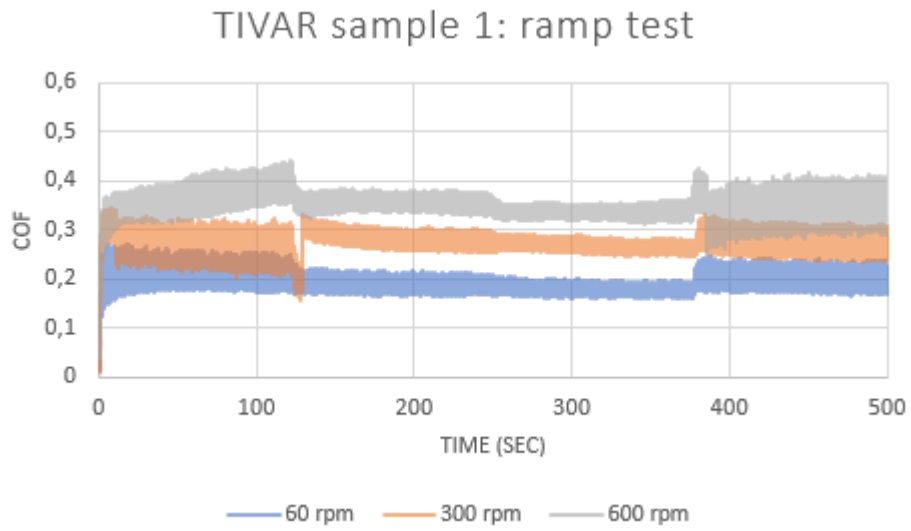

Figure 47. Tivar sample 1 ramp test with different loadings (20 N, 37 N, 54 N and 20 N) and with different speeds (60 rpm, 300 rpm and 600 rpm).

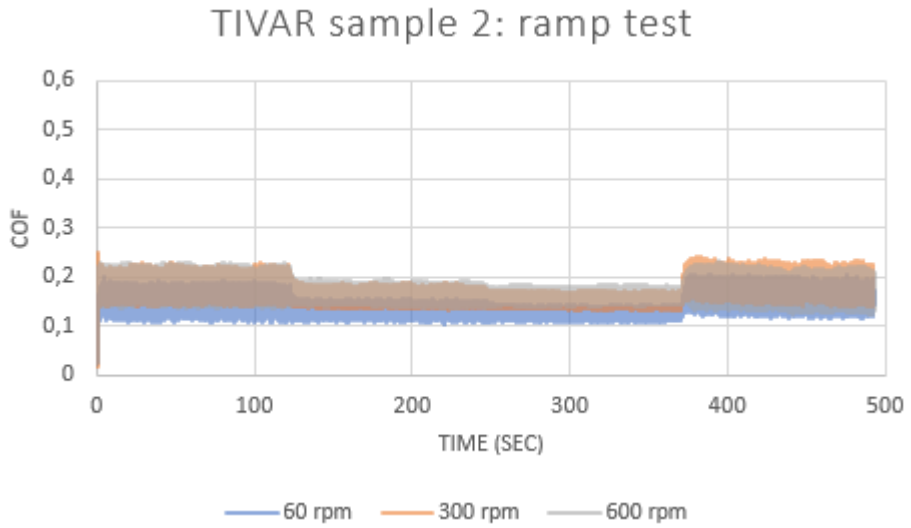

Figure 48. Tivar sample 2 ramp test with different loadings (20 N, 37 N, 54 N and 20 N) and with different speeds (60 rpm, 300 rpm and 600 rpm).

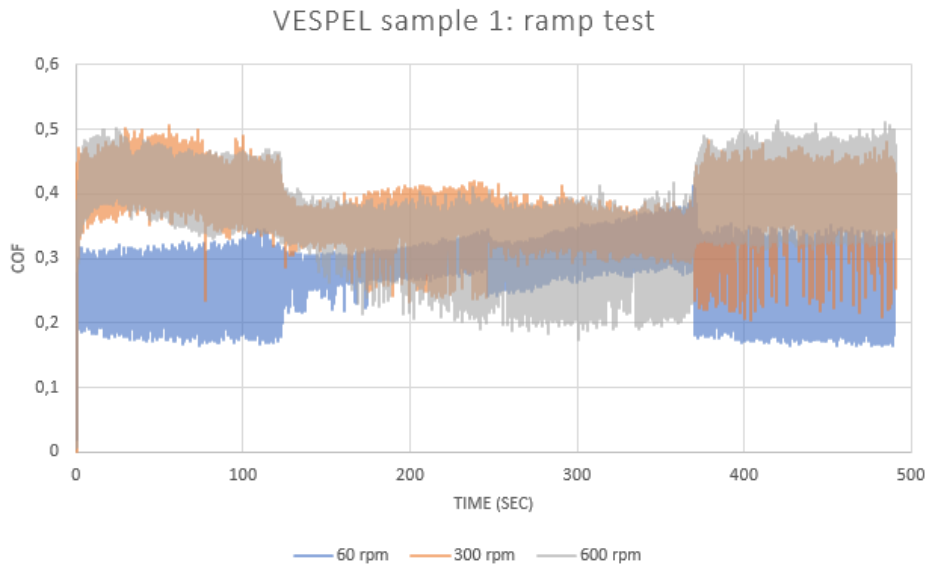

Figure 49. Vespel ramp test with different loadings (20 N, 37 N, 54 N and 20 N) and with different speeds (60 rpm, 300 rpm and 600 rpm)

In Table 14 and Figure 50, the average COF values for the ramp test with UTEC6540 are presented. Two parallel measurements were performed with two different samples. From Figure 50 it can be seen that the COF increases with increasing speed. By comparing results of 6000 rpm to 60 rpm, the COF increases approximately 54 % to 95 %. The increasing load does not seem to influence the COF at lower speeds (60 rpm and 300 rpm). At the higher speed of 600 rpm the highest load of 54 N has 20 % higher COF value compared to lower loadings.

The test starts with 20 N force and the force is increased gradually to 54 N. At the last step of the test, the loading is decreased back to 20 N to compare whether there is a difference in the COF in the end compared to the beginning of the test. With a lower speed of 60 rpm there is no difference. With higher speeds, the end of the test shows higher COF compared to the beginning. In the 300 rpm test, the increase in COF is 14 % and with 600 rpm test the increase of COF is 20 %. This can be explained by the frictional heating of the system. As the speed increases, more frictional heating is generated, which leads to thermal expansion and lower stiffness of the polymer sample increasing the real contact area resulting in increasing COF values.

Table 14. Average COF values from ramp test with UTEC6540 sample 1.

	60 rpm	300 rpm	600 rpm
20 N	0,21	0,27	0,34
37 N	0,22	0,27	0,34
54 N	0,21	0,27	0,41
20 N	0,21	0,31	0,41

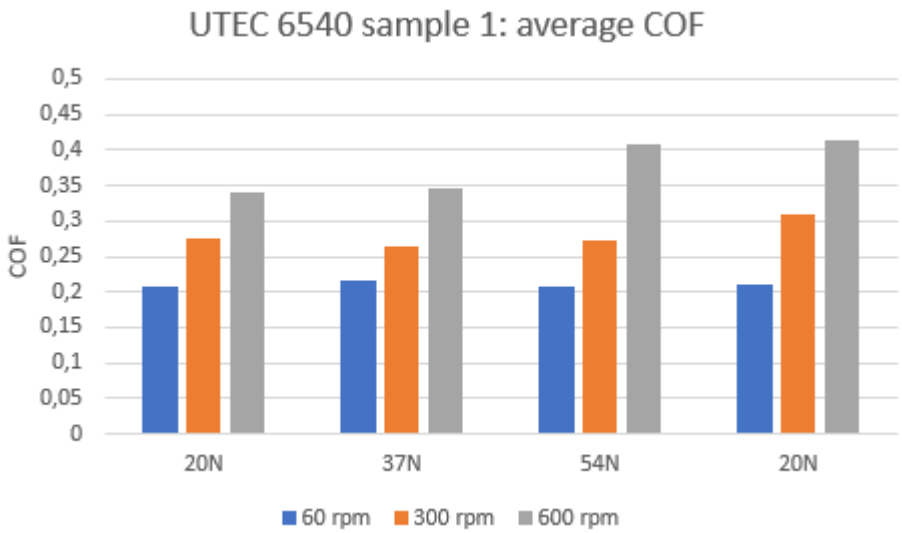

Figure 50. Average COF of UTEC6540 ramp tests with sample 1.

In Table 15 and Figure 51, the results of the ramp test with UTEC6540 sample 2 are presented. As seen in Figure 51, the trend is similar with the UTEC6540 sample 1. The average COF increases as the speed increases. With 600 rpm speed the COF increases 25 % to 66 % compared to the speed of 60 rpm. The COF with this sample decreases as the load increases with lower speeds of 60 rpm and 300 rpm 8 % to 18 %. With a higher speed of 600 rpm, the COF first decreases with 37 N loading (5 %) but with 54 N load COF increases slightly (12 %) compared to the testing with 20 N load.

Table 15. Average COF values from ramp test with UTEC6540 sample 2.

	60 rpm	300 rpm	600 rpm
20 N	0,32	0,39	0,40
37 N	0,28	0,34	0,38
54 N	0,26	0,33	0,41
20 N	0,27	0,36	0,45

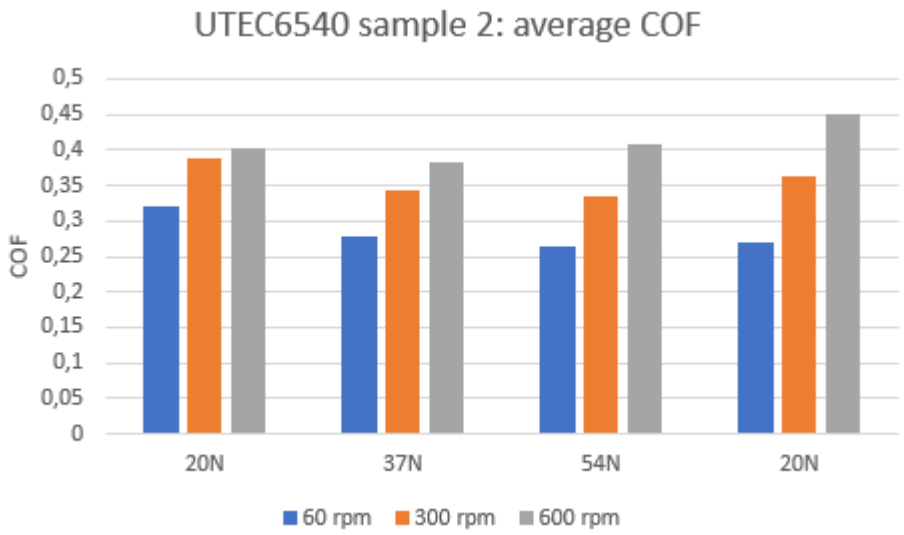

Figure 51. Average COF of UTEC6540 ramp tests with sample 2.

In Table 16 and Figure 52, the average COF values of the ramp test with PE1000R sample 1 are presented. As seen in Figure 52, the results show a similar trend compared to the UTEC6540 samples. As the speed is increased, the value of COF increases. With the speed of 600 rpm, the COF is 35 % to 42 % higher compared to the testing at speed of 60 rpm. As the load is increased, the value of COF decreases with all the different speeds. Comparing 54 N loading to 20 N loading, the COF decreases 4-10 %. When comparing the beginning (with 20 N loading) and the end of the test (with 20 N loading) there is a little difference (4 % increase) with 60 rpm speed, as well as with the 37 N load (8 % increase) and no difference with 54 N loading during the test.

Table 16. Average COF values from ramp test with PE1000R sample 1.

	60 rpm	300 rpm	600 rpm
20 N	0,21	0,24	0,29
37 N	0,20	0,23	0,27
54 N	0,19	0,23	0,27
20 N	0,22	0,26	0,29

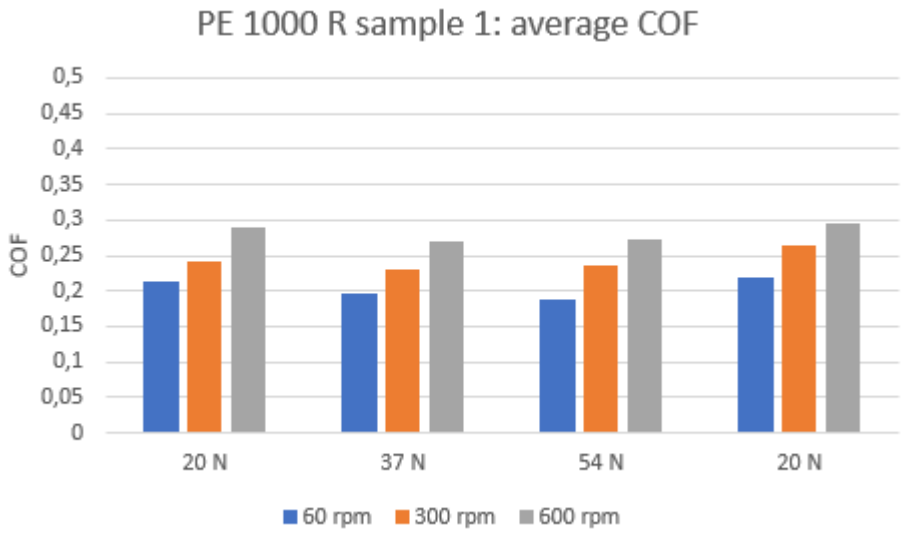

Figure 52. Average COF of PE1000R ramp tests with sample 1.

In Table 17 and Figure 53, the average COF values of the ramp test with Tivar sample 1 are presented. As seen in Figure 53, the increase in speed has a similar effect on the COF as on the other materials. As the speed is increased, the average COF increases 76-88 %. The increase in loading has also similar effect compared to the other materials. As the load is increased, the value of COF slightly decreases with the speeds of 60 rpm and 600 rpm (9-15 %). With 300 rpm speed, the value of COF first increases 7 % with 37 N loading compared to the 20 N loading but, with the 54 N loading, the value of COF is the same as with the 20 N load. When comparing the beginning of the test with the 20 N load to the end of the test with the same load, (with speeds of 60 rpm and 600 rpm) the average COF decreases 9-15 %. With 300 rpm test, the value of COF value slightly increases (4 %) in the end of test when compared to the start of test. This could indicate that there is less frictional heating or that the frictional heating has less effect on the stiffness of material.

Table 17. Average COF values from ramp test with Tivar sample 1.

	60 rpm	300 rpm	600 rpm
20 N	0,21	0,27	0,37
37 N	0,19	0,29	0,36
54 N	0,18	0,27	0,34
20 N	0,18	0,28	0,34

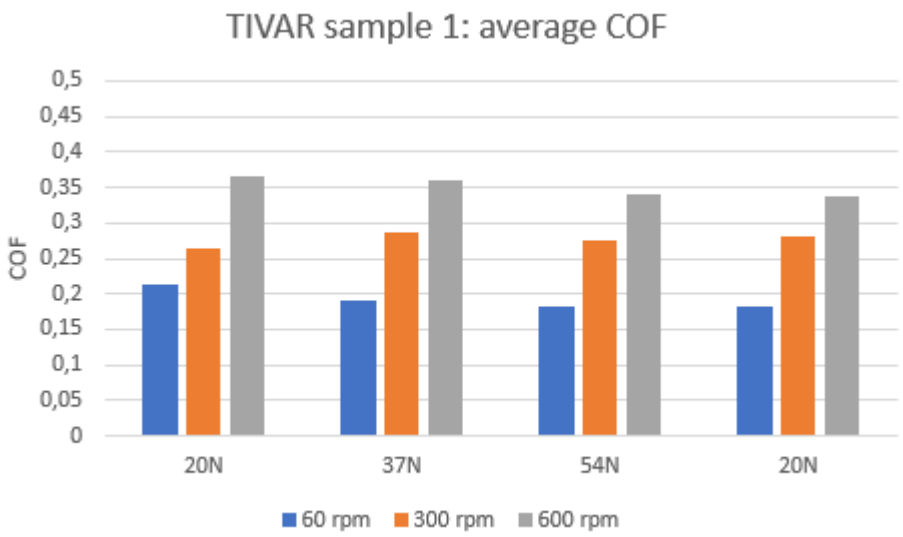

Figure 53. Average COF of Tivar ramp tests with sample 1.

In Table 18 and Figure 54, the average COF values of the ramp test with Tivar sample 2 are presented. This sample 2 has in general lower average COF values compared to the sample 1. However, the trend is the same as when comparing the effect of speed and load to the value of COF. With increasing speed, the COF value increases 20-30 %. By increasing the load, COF decreases 12-17 %. When comparing the beginning of the test with the 20 N load to the end of the test with the same load (with speeds of 60 rpm and 300 rpm) the value of COF increases 6-7 %. With the speed of 600 rpm, the value of COF remains.

Table 18. Average COF values from ramp test with Tivar sample 2.

	60 rpm	300 rpm	600 rpm
20 N	0,15	0,18	0,18
37 N	0,13	0,16	0,17
54 N	0,13	0,15	0,16
20 N	0,16	0,19	0,18

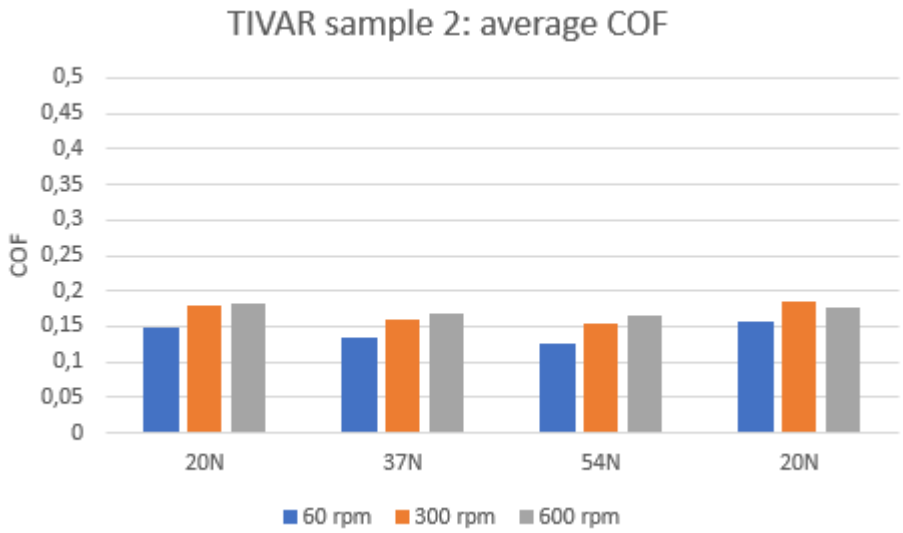

Figure 54. Average COF of Tivar ramp tests with sample 2.

In Table 19 and Figure 55, the average COF values from the ramp test with Vespel sample 1 are presented. The increase in speed increases the value of COF with 20 N loading by 50 %, with 37 N loading by 26 % and with 54 N loading by 3 %. The effect of increasing the loading with the lower speed of 60 rpm increases COF value by 15 %. With higher speeds, the value of COF is decreased 21-22 %. When comparing the beginning of the test with 20 N load to the end of the test with the same load (with 60 rpm and 600 rpm speeds) there is no observable difference. With 300 rpm speed, the value of COF decreases 14 % in the end of test compared to the beginning of the test.

Table 19. Average COF values from ramp test with Vespel sample 1.

	60 rpm	300 rpm	600 rpm
20 N	0,26	0,43	0,39
37 N	0,27	0,35	0,34
54 N	0,30	0,35	0,31
20 N	0,26	0,37	0,39

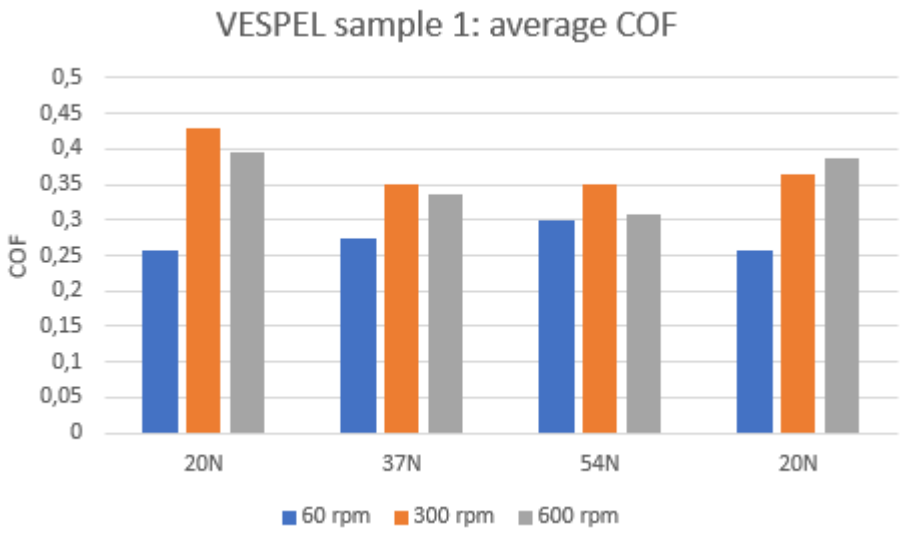

Figure 55. Average COF of Vespel ramp tests with sample 1.

In Table 20 and Figure 56, the average COF values with 54 N force and with the three different speeds (60 rpm, 300 rpm and 600 rpm) are presented for all the test sample series to make a comparison. From Figure 56, the trend of increasing speed leading to increasing COF can be seen with UTEC6540, PE1000R and Tivar series. In the ramp tests, again, it can be concluded, that the recycled material candidates (PE1000R and Tivar) have a lower COF compared to UTEC6540. The Vespel material series has higher COF value compared to UTEC6540 at the speeds of 60 rpm and 300 rpm, but a lower COF value with the high speed of 600 rpm. According to these results, Tivar has the lowest COF values in different test conditions.

Table 20. Average COF values of ramp test with 54 N force and with different speeds (60 rpm, 300 rpm and 600 rpm).

Sample	60 rpm	300 rpm	600 rpm
UTEC6540	0,26	0,33	0,41
PE1000R	0,19	0,23	0,27
TIVAR	0,16	0,22	0,25
VESPEL	0,30	0,35	0,31

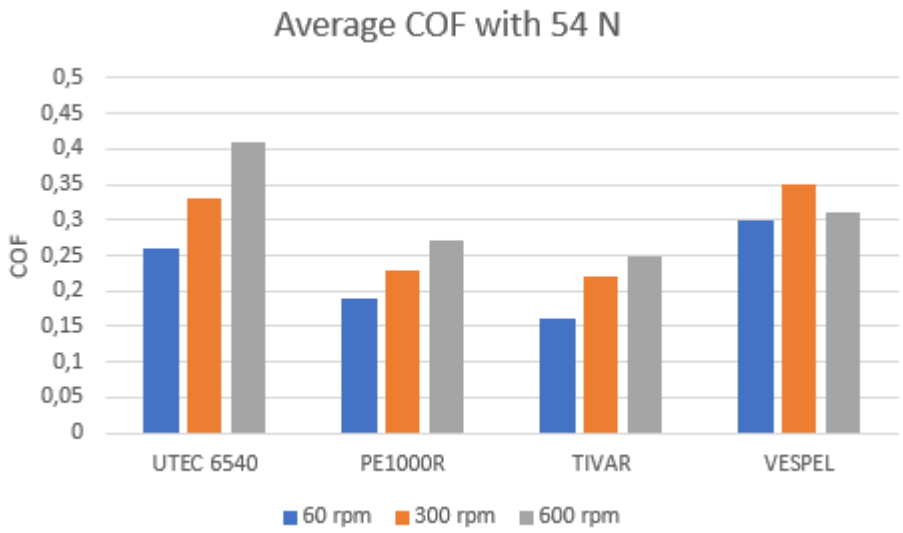

Figure 56. Comparison of average COF for material series using the ramp test with 54 N force and with different speeds (60 rpm, 300 rpm and 600 rpm).

The wear of the samples was observed by the height change during the measurement. The device records the vertical height change of the pin as the pin wears. The carriage of the test device moves down as the pin wears to maintain the constant loading on the pin. This is the height change recorded in this thesis. The tests were too short to gain reliable results of the wear rates, therefore the wear results are not presented. In Figure 57, Figure 58, Figure 59, and Figure 60 the pictures of the worn samples are presented. In the pictures it can be seen, that, typically, the whole surface of the pin has not been in contact with the disk, thus the real contact surface has been smaller than the surface area of the pin especially in case of UTEC6540 (see Figure 57) and Vespel (see Figure 60) samples. The samples of PE1000R and Tivar show a more uniform grooves across the surface of the pin (see Figure 58 and Figure 59).

Figure 57. Worn samples of UTEC6540.

Figure 58. Worn samples of PE1000R.

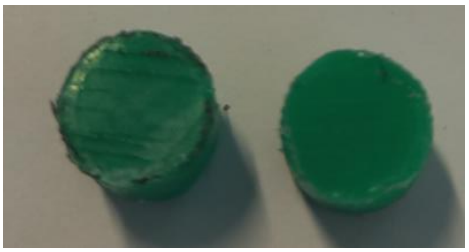

Figure 59. Worn samples of Tivar.

Figure 60. Worn samples of Vespel.

In Figure 61, Figure 62, Figure 63, and Figure 64, the pictures of the disks after the test are presented. There are some grooves on the disks along the path of the polymer pin. However, there is no polymer attached to the disks by visual observation.

Figure 61. Worn disk after testing with UTEC6540.

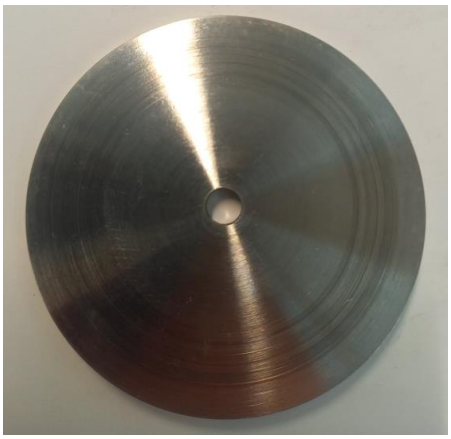

Figure 62. Worn disk after testing with PE1000R.

Figure 63. Worn disk after testing with Tivar.

Figure 64. Worn disk after testing with Vespel.

5.3.2 Measurements with a wet contact surface

Tests with water as a lubricant were conducted to get an idea of how lubrication effects the COF values. The lubricated tests were done as a 30-minute test with a 60 rpm speed

and with a 54 N force. 14 mL of water was used as lubricant. The amount of water covered the whole surface of the disk and the pin and disk interface remained submerged in water the whole duration of the test. The results of the tests are presented in Figure 65, Figure 66, Figure 67, and Figure 68.

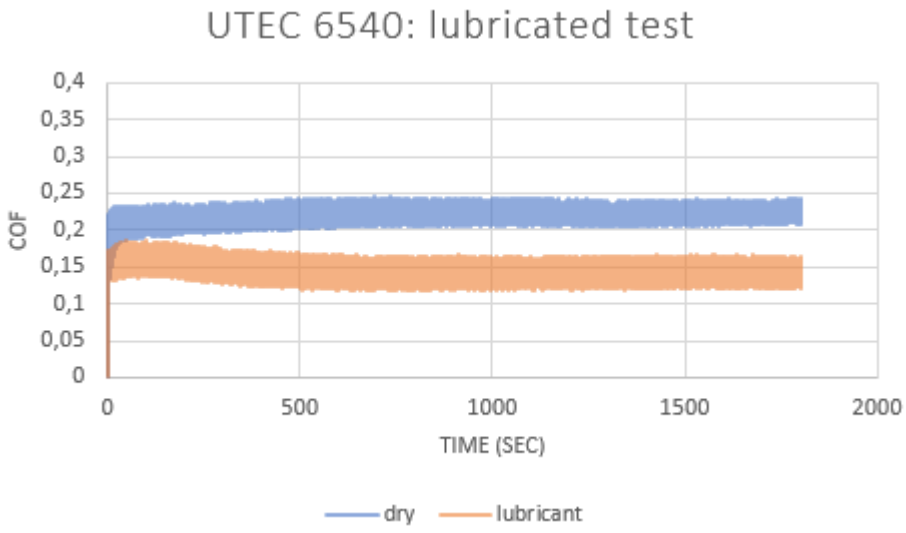

Figure 65. Results of dry and lubricated tests with UTEC6540 series.

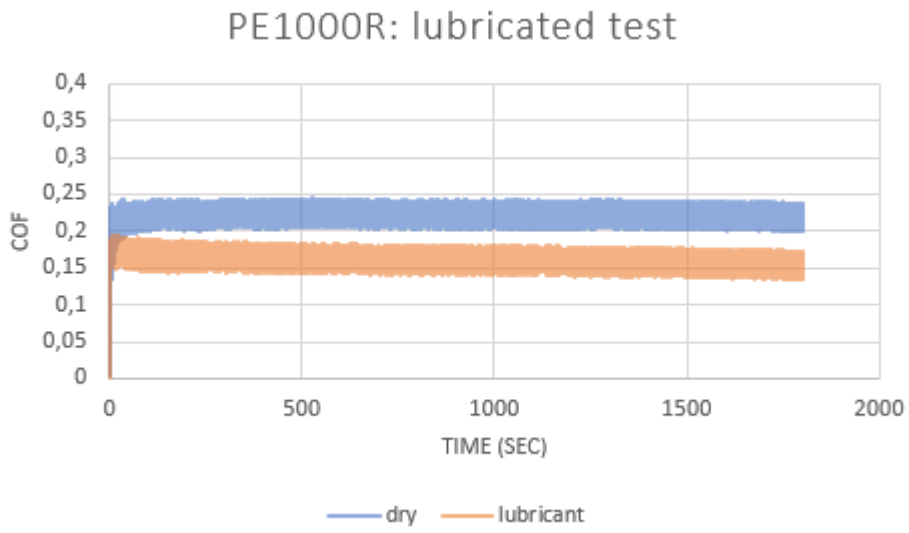

Figure 66. Results of dry and lubricated tests with PE1000R series.

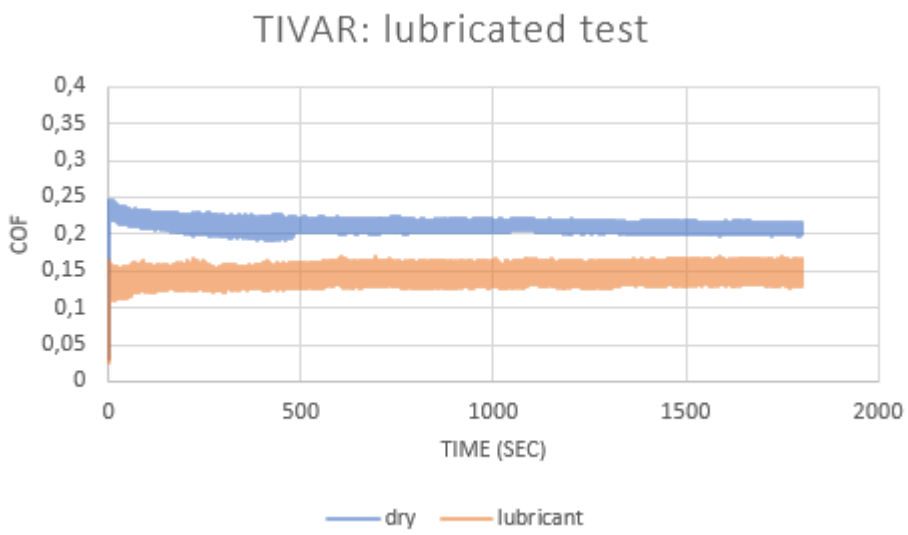

Figure 67. Results of dry and lubricated tests with Tivar series.

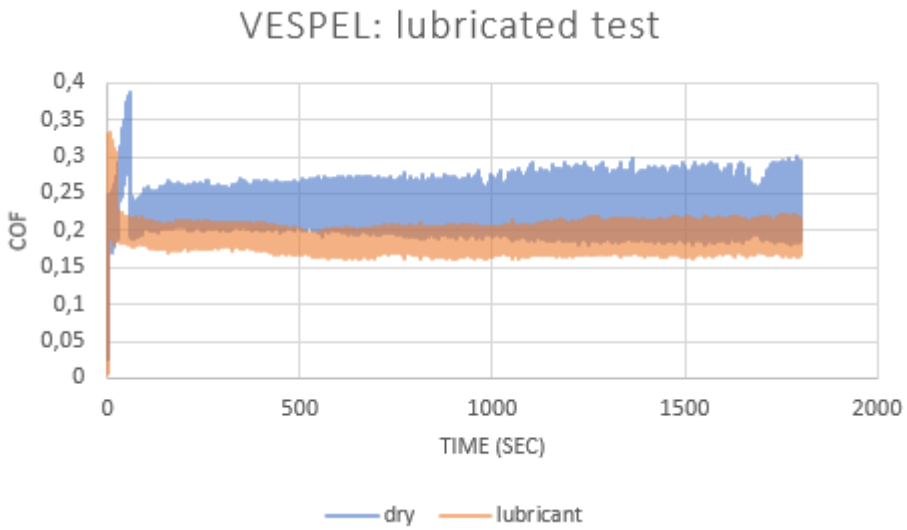

Figure 68. Results of dry and lubricated tests with Vespel series.

In Table 21 and Figure 69, the average COF values for the dry and lubricated tests with 60 rpm speed and 54 N load are presented. With all the samples tested in this thesis, the lubricated tests show lower COF values, as seen in Figure 69. The difference of lubricated contact compared to dry contact is between 25-32 %. In the dry test, Tivar has the lowest COF (0,21), which is 5 % lower compared to UTEC6540. Vespel sample has the highest COF (0,24), which is 9 % higher than UTEC6540. PE1000R has the same COF as UTEC6540 (0,22). In the wet contact testing, the lowest COF value is measured with UTEC6540 and Tivar (0,15). The highest COF in the lubricated condition is measured with Vespel (0,18), which is 20 % higher than with UTEC6540. PE1000R has COF in between the highest and lowest (0,16), which is 6,7 % higher than with UTEC6540. In conclusion, the material pair of polymer and steel with series of this thesis show

decreased COF values when the contact surface is lubricated with water. When comparing the different materials, Vespel shows the highest average COF both in dry and wet contact testing. The three other materials (UTEC6540, PE1000R and Tivar) seem to have similar average COF values in these test conditions.

Table 21. Average COF values of dry and lubricated tests with 60 rpm speed and 54 N load for 30 minutes.

Sample	Dry	Lubricant	Change in COF (%)
UTEC6540	0,22	0,14	64,5
PE1000R	0,22	0,16	74,4
TIVAR	0,21	0,15	70,5
VESPEL	0,24	0,18	77,8

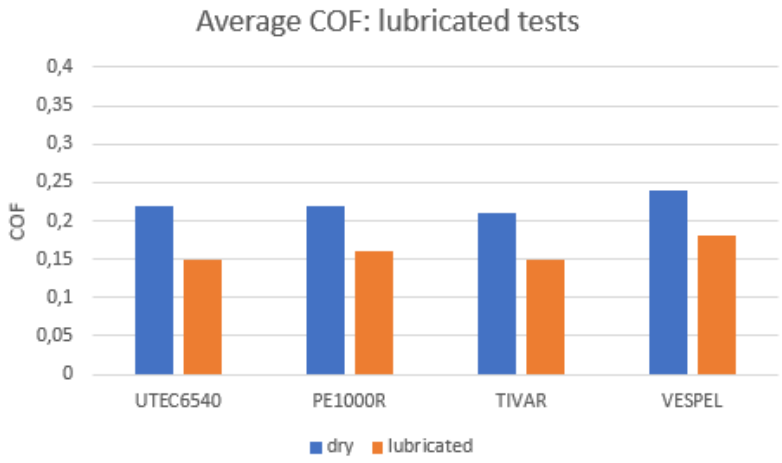

Figure 69. Average COF values in dry-wet contact conditions.

The pictures of the worn samples after the dry-wet contact tests are presented in Figure 70. From the pictures it can be seen, that the real contact surface has not been the whole surface of the pin, but the pin shows grooves only in part of the surface of the pin. This means that the contact pressure has varied with regard to the anticipated pressure based on the test load.

Figure 70. Worn samples of UTEC6540, PE1000R, Tivar and Vespel with lubricated contact.

6. DISCUSSION

6.1 Tensile tests - notes

In Table 22, the average results of the tensile tests for UHMWPE materials are presented including average values for UHMWPE material properties found in the current literature. The Young's modulus results of UHMWPE (UTEC6540, PE1000R and Tivar) are 37,3 % to 44,5 % lower compared to the Young's modulus value in literature. Also, the tensile strength are lower compared to the literature: strength at yield results of the UHMWPE samples are 17,0 % to 25,3 % lower compared to the values in the literature for UHMWPE. Tensile of UTEC6540, PE1000R and Tivar are 19,6 % to 53,6 % lower than the average values from the literature. The elongation at break values from the tests are also lower compared to the average values from the literature: 37,0 % to 72,1 % lower compared to the literature values. The elongation at yield values of the tests agree better the average values given in the literature: the test result of UTEC6540 was 0,8 % less compared to the literature, PE1000R and for Tivar results are 5,3 % and 19,2 % higher compared to the values in the literature.

Table 22. Mechanical properties of UHMWPE from the current literature compared to the tensile test results of UTEC6540, Pe1000R and Tivar in this thesis. (literature reference: Dielectric Manufacturing, 2021)

Property	UHMWPE (literature)	UTEC6540	PE1000R	TIVAR
Young's modulus (MPa)	894-963	553,1	515,5	581,8
Strength at yield (MPa)	21,4-27,6	18,29	19,26	20,33
Tensile strength (MPa)	38,6-48,3	20,15	34,95	25,84
Elongation at yield (%)	11	10,91	11,58	13,11
Elongation at break (%)	350-525	122,1	275,8	197,7

In Table 23, Table 24, and Table 25, the tensile test results of UHMWPE test series (UTEC6540, PE1000R and Tivar are compared to the manufacturers reported mechanical property values. In Table 23, UTEC6540 test results are compared. The yield strength corresponds to the reported value in this thesis. Tensile strength reported in this thesis is 32,8 % lower than reported and elongation at break 65,1 % lower than reported in this thesis. (Braskem, 2018)

Table 23. Mechanical properties of UTEC6540 from the current literature compared to the tensile test results of UTEC6540 in this thesis. (literature reference: Braskem, 2018)

Property	UTEC6540 (literature)	UTEC6540 (tested)
Strength at yield (MPa)	>17	18,29
Tensile strength (MPa)	>30	20,15
Elongation at break (%)	350	122,1

In Table 24 the results of PE1000R test results are compared to the mechanical properties reported by the manufacturer. Young's modulus was tested to be 42,7 % lower than reported, tensile strength in this thesis 29,4 % higher than reported by manufacturer and elongation at break was 37,9 % higher than reported by the manufacturer.

Table 24. Mechanical properties of PE1000R from the current literature compared to the tensile test results of PE1000R in this thesis. (literature reference: Wefapress, 2020)

Property	PE1000R (literature)	PE1000R (tested)
Modulus (MPa)	900	515,5
Tensile strength at break (MPa)	27	34,95
Elongation at break (%)	200	275,8

In Table 25, the results of Tivar series are compared to the mechanical properties reported by the manufacturer. Young's modulus was tested in this thesis to be 16,9 % lower than reported by the manufacturer, strength at yield in this thesis 3,2 % lower than reported by manufacturer and elongation at yield 5,3 % higher than reported by manufacturer. The test results in this thesis of Tivar correspond very well the values given by the manufacturer.

Table 25. Mechanical properties of Tivar from the current literature compared to the tensile test results of Tivar in this thesis. (literature reference: Bay Plastics Datasheet, 2022)

Property	Tivar (literature)	Tivar (tested)
Young's modulus (MPa)	700	581,8
Strength at yield (MPa)	21	20,33
Elongation at yield (%)	11	11,58

In Table 26, average results of tensile testing of Vespel series are compared to polyimide material properties found in the current literature. The Young's modulus measured for Vespel in this thesis is 13,6 % less compared to the literature value. Tensile strength in this thesis is 40,4 % less compared to the literature value. The elongation at break in this thesis is 19,3 % more compared to the literature value. The Vespel series specimens were prepared grinding by hand, thus the shape of the test specimens was not as precise as with the punched samples. This may have influenced the tensile test results.

Table 26. Mechanical properties of polyimide from the current literature compared to tensile test results of Vespel in this thesis. (literature reference: Aikolon, 2000)

Property	Polyimide (literature)	Vespel
Young's modulus (MPa)	3600	3109
Strength at break (MPa)	116	69,1
Elongation at break (%)	3,8	4,5

In conclusion, the Vespel series in this thesis has higher modulus and higher tensile strength at break compared to the other series (UTEC6540, PE1000R and Tivar). Vespel is also more brittle compared to the UHMWPE series, which show tough behaviour. From the UHMWPE series, Tivar has the highest Young's modulus and strength at yield - making it the most potential replacement option.

6.2 Dynamic mechanical testing - notes

The temperature control in the DMA tests happens based on the thermocouple positioned near the sample, which corresponds to the sample temperature (T_s) and a thermocouple in the clamps (T_{ca}). The device tries to balance these two temperatures, but during the tests, there were some problems with the temperature control. When trying to reach the start temperature (in this case -55 Cº), the device had difficulties of reaching the correct temperature before starting the measurement. Thus, the temperature range of samples differ from each other for some amount.

6.3 Pin-on-Disk tests - notes

In the pin-on-disk tests, the materials were tested in terms of coefficient of friction in longer test with constant load and speed, in ramp tests with changing load and speed and with a water lubricant. In conclusion, Tivar series performed best showing lowest average coefficient of friction of the series. The Vespel series showed highest coefficient

of friction on average making it the poorest material regarding a target of low friction in the test conditions in this thesis.

The sample pin is positioned in the sample holder with screws and the position is evaluated by the naked eye. The pin should be parallel to the disk surface to get the contact area as close as possible to the theoretical contact area. In practice, the real contact area is always less than the theoretical contact area, meaning that the contact pressure is not exactly the one anticipated based on the device load and area of the pin contact.

During the test, the friction causes frictional heating in the contact surface. This can cause thermal expansion of the polymer and lower stiffness affecting the Z values (height difference) of the measurement. Frictional heating can also cause the polymer to stick to the disk, which results in polymer-polymer contact surfaces. This can influence the COF values when the material couple is not polymer on metal, but rather polymer on polymer.

7. CONCLUSIONS

According to the studies in this thesis, polyimide (Vespel series) has higher Young's modulus and higher tensile strength at break compared to the UHMWPE candidate materials tested (UTEC6540, PE1000R and Tivar). Polyimide is also more brittle in its tensile behaviour compared to the UHMWPE candidates. From the different UHMWPE series differentiated by the manufacturer of the test pieces, Tivar provided material that indicated the highest Young's modulus and strength at yield making it the most potential option to replace the current rival UHMWPE material (UTEC6540).

Regarding the DMA analysis, Polyimide shows highest storage modulus indicating it is the stiffest material in this thesis. From the UHMWPE series, the material provided by Tivar showed the highest storage modulus, 20 % higher compared to the rival material (UTEC6540).

When comparing the results gained from the friction tests (pin-on-disk), the material provided by Tivar tended to be the best option for the application of target in this thesis, owing to its low friction coefficient values. However, its wear resistance might not be as good as the wear resistance of polyimide, which has a high Young's modulus and ultimate strength. Among the candidate UHMWPE material series, the material provided by Tivar is the best option for application as a replacement according to this thesis: the series was tested to have higher tensile modulus and tensile strength including higher storage modulus throughout the temperature range tested by using DMA (from -55 Cº to 120 Cº).

REFERENCES

Aikolon. (2000). PI (polyimide). Available at: https://www.aikolon.fi/en/products/high-performance-plastics/pi

Aikolon. (2019). UHMW-PE – Ultra-high-molecular-weight-polyethylene – PE 1000 R. Available at: https://www.aikolon.fi/en/products/volume-plastics/pe-1000-r

H, Alhazmi, F. H. Almansour, Z. Aldhafeeri. (2021). Sustainability Plastic Waste Management: A Review of Existing Life Cycle Assessment Studies, Sustainability 13, no. 10: 5340. Available at: https://doi.org/10.3390/su13105340

L. Baürle, D. Szaboá, M. Fauve, H. Rhyner, N. D. Spencer. (2006). Sliding friction of polyethylene on ice: tribometer measurements, Tribol Lett 24, p. 77–84. Available at: https://doi.org/10.1007/s11249-006-9147-z

Bay Plastics Datasheet. (2022). PE1000 Regenerated Sheet – Pressed & Planed.

Braskem. (2016). Braskem UTEC. Available at: https://www.braskem.com.br/utec

Braskem. (2018). Ultra High Molecular Weight Polyethylene, Braskem America Inc.

T. R. Crompton. (2013). Thermal methods of polymer analysis, Smithers Rapra Technology.

Dielectric Manufacturing. (2021). UHMW (Ultra-High-Molecular-Weight-Polyethylene). Available at: https://dielectricmfg.com/knowledge-base/uhmw/

C. Dyson, A. Azam. (2020). Webinar Series on the Fundamentals and Application of Tribology: Friction. Institution of Mechanical engineers. Available at: https://www.youtube.com/watch?v=dVeqFxAe_bc

W. F. Hosford. (2010). Mechanical behavior of materials, Cambridge university press.

ISO. (2018). ISO 14855-2:2018. Determination of the ultimate aerobic biodegradability of plastic materials under controlled composting conditions — Method by analysis of evolved carbon dioxide — Part 2: Gravimetric measurement of carbon dioxide evolved in a laboratory-scale test. Available at: https://www.iso.org/standard/72046.html

D. Ita-Nagy, I. Vázquez-Rowe, R. Kahhat, G. Chinga-Carrasco, I. Quispe. (2020). Reviewing environmental life cycle impacts of biobased polymers: current trends and methodological challenges, The International Journal of Life Cycle Assessment 25.11, p. 2169-218. Available at: https://doi.org/10.1007/s11367-020-01829-2

R. L. Jackson. (2012). Handbook of Lubrication and Tribology, Volume II : Theory and Design, Second Edition. Handbook of Lubrication and Tribology, Volume II: Theory and Design, Second Edition. Available at: https://doi.org/10.1201/B12265

Y. Kikuchi, M. Hirao, K. Narita, E. Sugiyama, S. Oliveira, S. Chapman, M. M. Arakaki, C. M. Cappra. (2013). Environmental Performance of Biomass-Derived Chemical Production: A Case Study on Sugarcane-Derived Polyethylene. Journal of chemical engineering of Japan 46.4, p. 319–325.

H. Kuhn, D. Medlin. (2000). Mechanical Testing and Evaluation, ASM International, p. 26–48. Available at: https://doi.org/10.31399/ASM.HB.V08.A0003256

Mettler-Toledo AG. (2010a). Interpreting DMA curves Part 1. Mettler Toledo Thermal Analysis UserCom 15.

Mettler-Toledo AG. (2010b). Tips on method development for DMA measurements in 3-point bending. Mettler Toledo Thermal Analysis UserCom 28.

L. W. McKeen. (2010). Fatigue and Tribological Properties of Plastics and Elastomers, 2nd Edition, Fatigue and Tribological Properties of Plastics and Elastomers, 2nd Edition. Available at: https://doi.org/10.1016/C2009-0-20351-5

N. K. Myshkin, A. V. Kovalev. (2009). Adhesion and Friction of Polymers, Polymer Tribology, p. 3–37.

C. Stamboulides, P. Englezos, S. G. Hatzikiriakos. (2012). The ice friction of polymeric substrates, Tribology International, 55, p. 59–67. Available at: https://doi.org/10.1016/J.TRIBOINT.2012.05.001

Tampere University. (2022). Thermal analysis of materials. Available at: https://www.tuni.fi/en/research/thermal-analysis-materials#expander-trigger--7f3c5fca-23eb-459b-be2d-a66411437fb9

H. Unal, U. Sen, A. Mimaroglu. (2004). Dry sliding wear characteristics of some industrial polymers against steel counterface, Tribology International, 37(9), p. 727–732. Available at: https://doi.org/10.1016/J.TRIBOINT.2004.03.002

H. Unal, S. H. Yetgin, F. Findik. (2014). The effect of applied load and sliding speed on the tribological properties of Nylon 6 and ultra-high-molecular-weight polyethylene, Industrial Lubrication and Tribology, 66(3), p. 498–504. Available at: https://doi.org/10.1108/ILT-10-2011-0082

Y. Q. Wang, J. Li. (1999). Sliding wear behavior and mechanism of ultra-high molecular weight polyethylene, Materials Science and Engineering: A, 266(1–2), p. 155–160. Available at: https://doi.org/10.1016/S0921-5093(99)00040-4

Wefapress. (2020). Technical Data Sheet – A4 ®.

APPENDIX 1: FORCE OFFSET, DISPLACEMENT AMPLITUDE AND FORCE AMPLITUDE PRETEST FOR DMA ANALYSIS

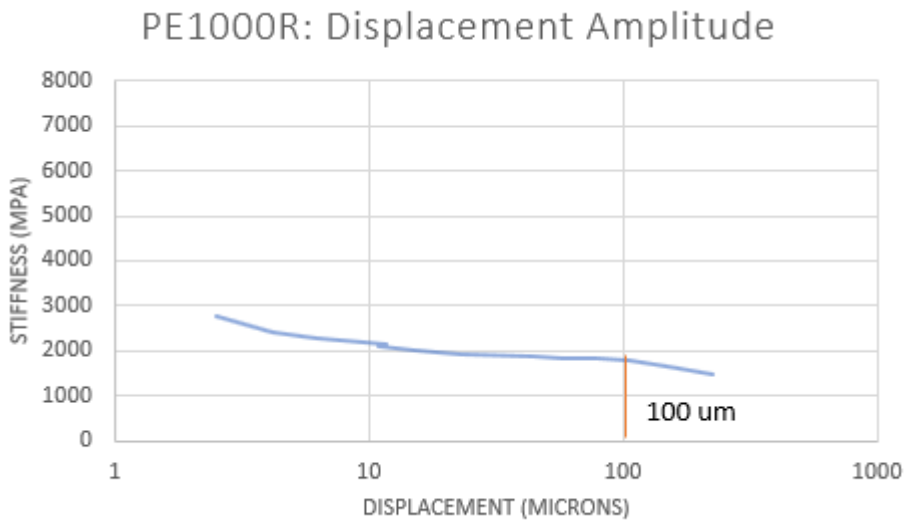

Figure 71. Results for displacement amplitude (DA) pretest for PE1000R series.

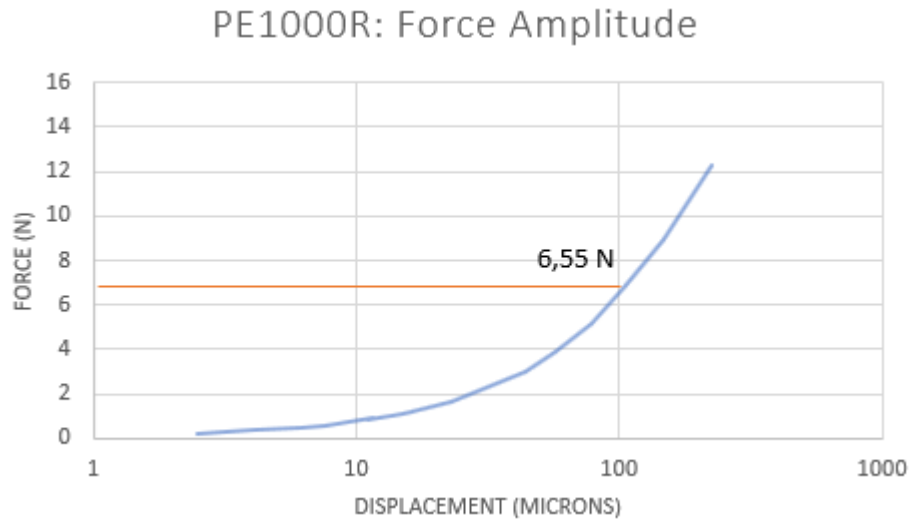

Figure 72. Results for force amplitude (FA) pretest for PE1000R series.

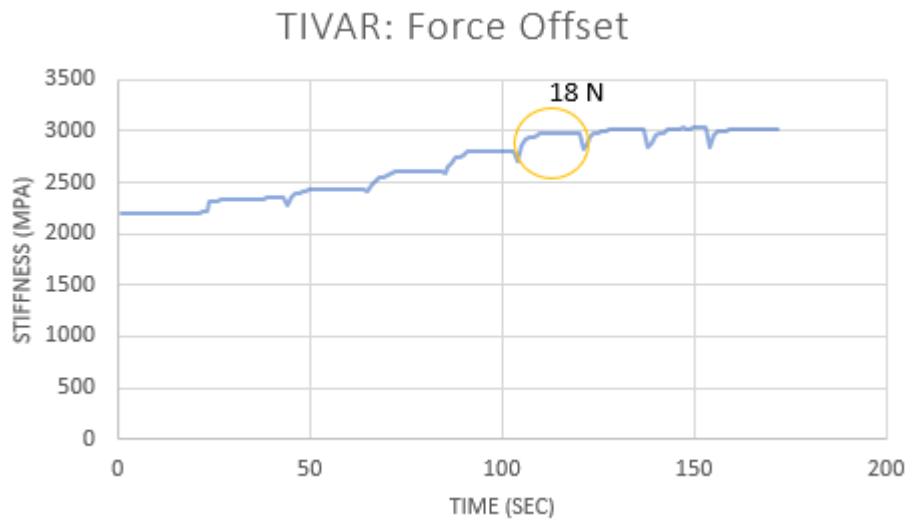

Figure 73. Force Offset (FO) pretest results of Tivar series.

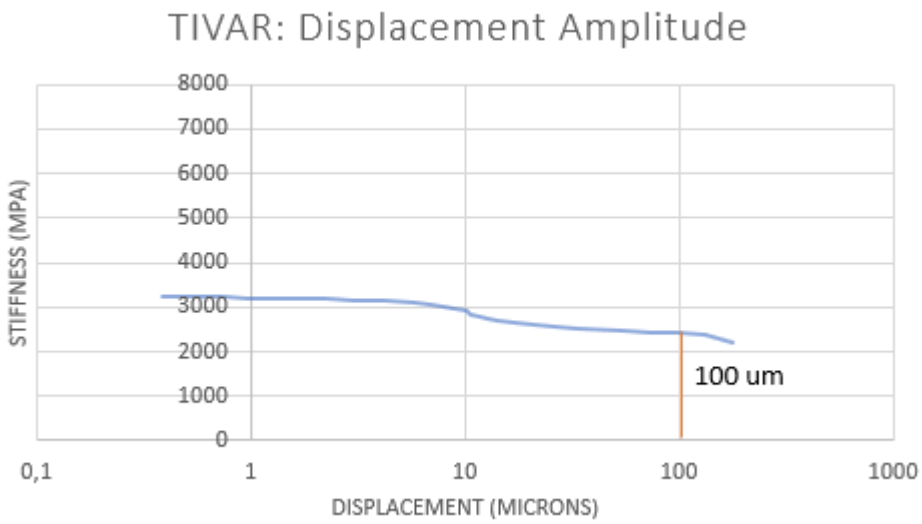

Figure 74. Displacement amplitude (DA) pretest results of Tivar series.

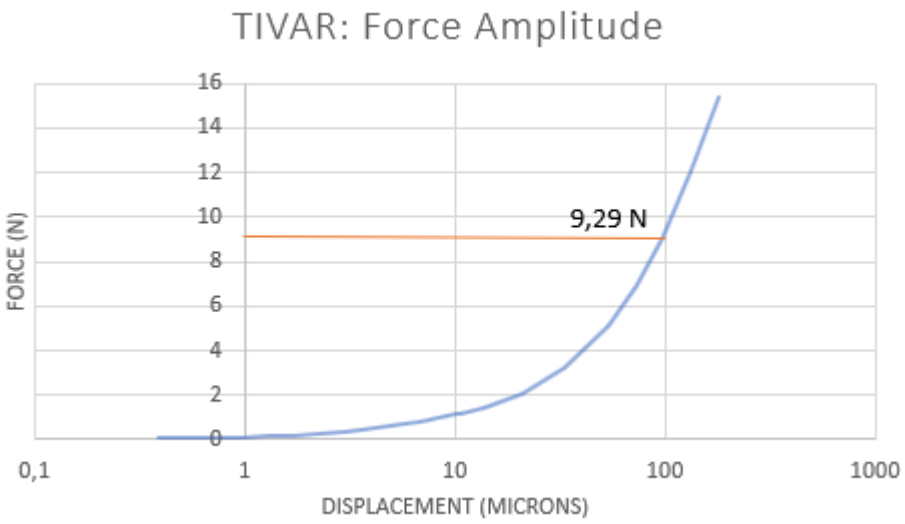

Figure 75. Force amplitude (FA) pretest results of Tivar series.

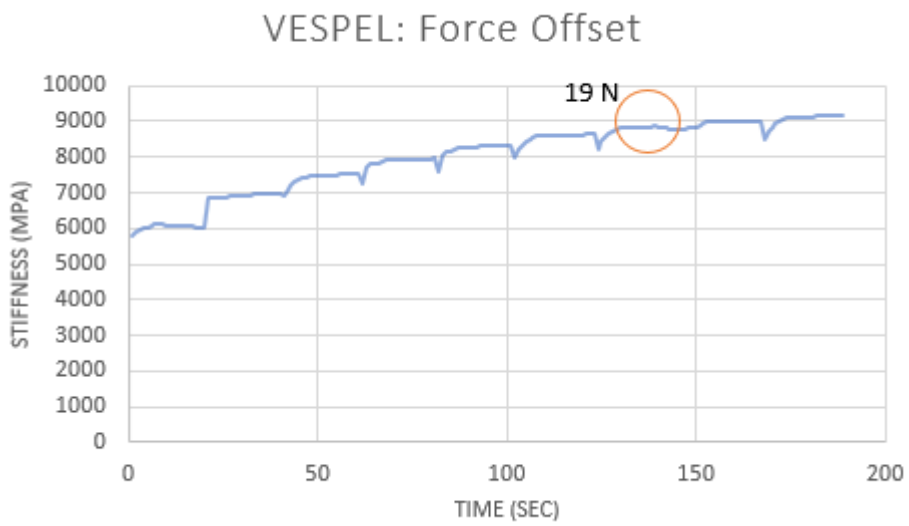

Figure 76. Force Offset pretest (FO) with Vespel series.

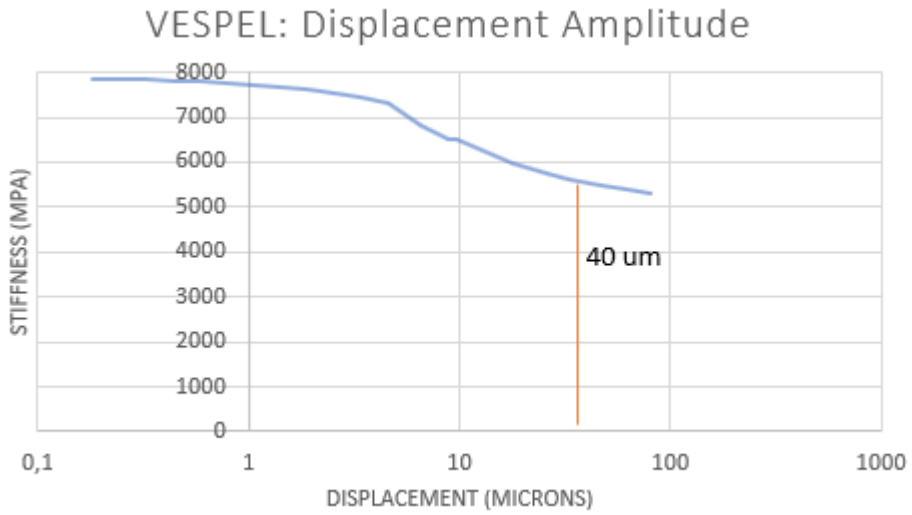

Figure 77. Results for displacement amplitude (DA) pretest for Vespel series.

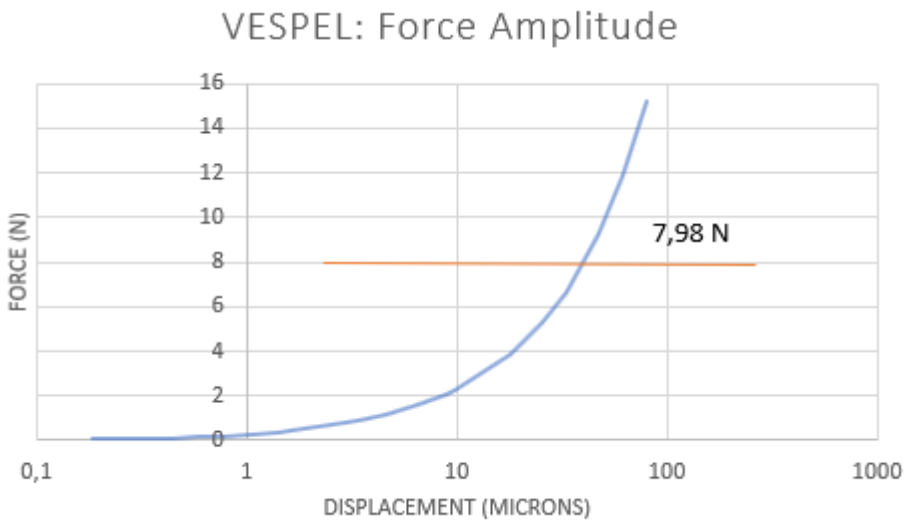

Figure 78. Results for force amplitude (FA) pretest for Vespel series.